Catalytic Promiscuity of Cytochrome c towards Proton Transfer Reaction

Sheetal Rani

MS15164

A dissertation submitted for the partial fulfilment of

BS-MS dual degree in science

Indian Institute of Science Education and Research Mohali

May 2020

Certificate of Examination

This is to certify that the dissertation titled “Catalytic promiscuity of cytochrome c towards proton transfer reaction” submitted by Sheetal Rani (Reg. No. MS15164) for the partial fulfilment of BS-MS dual degree programme of the institute, has been examined by the thesis committee duly appointed by the institute. The committee finds the work done by the candidate satisfactory and recommends that the report be accepted.

Dr. Subhabrata Maiti (Supervisor) Dr. Sabyasachi Rakshit Dr. Sugumar Venkataramani

Dated: 4th May, 2020

Declaration

The work presented in this dissertation has been carried out by me under the guidance of Dr. Subhabrata Maiti at the Indian Institute of Science Education and Research Mohali.

This work has not been submitted in part or in full for a degree, a diploma, or a fellowship to any other university or institute. Whenever contributions of others are involved, every effort is made to indicate this clearly, with due acknowledgement of collaborative research and discussions. This thesis is a bonafide record of original work done by me and all sources listed within have been detailed in the bibliography.

Sheetal Rani

(Candidate)

Dated: 4th May, 2020

In my capacity as the supervisor of the candidate's project work, I certify that the above statements by the candidate are true to the best of my knowledge.

Dr. Subhabrata Maiti

(Supervisor)

Acknowledgements

I would like to express deepest gratitude towards my supervisor, Prof. Subhabrata Maiti for giving me the chance to work with him and providing all the facilities required to complete this desertion. I am extremely grateful and indebted to him for his expert, sincere, valuable guidance throughout the course of this project.

I would also like to thanks my committee members Dr. Sabyasachi Rakshit and Dr. Sugumar Venkataramani for their insightful comments and suggestions during this project work.

I owe my special thanks to Dr. Kalpana Tomar and Basundhara Dasgupta for being always available for me anytime, also they helped and supported me in all circumstances.

I would like to thanks other fellow lab members Ekta, Akshi, Priyanka, Rishi and Himanshu for being very helpful and for maintaining a friendly, cheerful and peaceful atmosphere in the Lab. You all supported me greatly and were always willing to help me. It has always been a pleasure to come to lab every day with such a lovely and dedicated people.

Last but not least, I would like to thanks the most important people in my life, my parents Mr Jagat Singh and Mrs Rajeshwari for their love, endless support and motivation in every situation of my life. My dearest thanks to my siblings, most valuable gifts of my life, for always being there for me as friend. I am always indebted to my family for giving me the opportunities and experiences that have made me who I am. To all my friends, thank you for your support and help in my many many moments of crisis. Your friendship makes my life a wonderful experience. Thanks, too, to anyone I've forgotten who was instrumental in this project.

Table of Contents

List of Figures

List of Tables

List of Abbreviations:

Cyt c	Cytochrome c
NBI	5-nitrobenzisoxazole
2-CNP	2-Cyano-4-nitrophenol
CMC	Critical Micelle Concentration
KE	Kemp Elimination
DEPC	Diethylpyrocarbonate
GdnCl	Guanidinium hydrochloride
FITC	Fluorescein isothiacyanate
BSA	Bovine Serum Albumin
HSA	Human Serum Abumin
HRP	Horseradish Peroxidase

Abstract

In this study we have investigated the ability of cytochrome c (cyt c) as a catalyst for proton transfer reaction. Cyt c is small, globular heme protein having molecular weight ~12500. It is most primitive omnipresent protein which is present in all forms of aerobic organisms as well as in some anaerobic organisms. Here it is worthy to mention that the proteins/enzymes evolved in the early days of the evolutionary processes may possess wider range of substrate specificity to carry out multiple tasks as compared to the recently evolved enzymes. Apart from its primary function as an electron transporter in respiratory chain, cyt c is also known for its peroxidative property in lipid membrane by exposing heme moiety (its tertiary gets unfolded in membrane mimetic media) to the substrate. This now enables the peroxide substrate to bind with iron centre to show its peroxidase property. This made us curious to investigate the proton transfer ability of cyt c and fortunately, we have found that cyt c shows catalytic promiscuity towards proton transfer reaction, but this effect is strictly restricted to membrane mimetic media such as micelles and vesicles. Other enzymes/proteins like Lipase, Alkaline Phosphatase, Haemoglobin, HRP, catalase and lysozyme were also tested for proton transfer catalysis but none of them showed any catalytic rate.

5-nitrobenzisoxazole (NBI) was used as model substrate to study proton transfer by following Kemp elimination reaction. The catalytic rate by cyt c is found to increase with its residence at hydrophobic environment and also with the degree of unfolding of cyt c. The proximal histidine (His-18) moiety near hemin group is might be acting as base and responsible for the abstraction of proton from NBI (substrate) to form 2-CNP (product). Interestingly, In comparison with the aqueous buffer we have found approximately 250-fold increased KE catalysis by cyt c. As a whole, unprecedented catalytic promiscuity of cyt c towards proton transfer reaction has been found in this study, which can be highly significant in the evolutionary context, taking into consideration its role in delineating phylogenetic tree and also for producing biocatalyst with programmable multi-functional properties.

Chapter 1

Introduction

1.1. Biocatalysis:

It is the process in which biological enzymes / proteins are used as catalyst to accelerate the chemical reactions. Many new brilliant catalysts have been created by nature with evolution. It mostly includes proteins and nucleic acid with catalytic properties similar to the enzymes found in 80s.[1] Enzymes play crucial role in the catalysis of many chemical reactions; they speed up the chemical reaction by reducing the activation energy, without changing the equilibrium of the reaction.

There are many Reactions known to catalysed by biological substances, one such example is Kemp elimination reaction which is catalysed by a natural protein i.e. Serum Albumins.

Recent advances in scientific research have contributed to the understanding of enzyme structure and functioning leading to greater stability, activity, sustainability and substrate specifity. At present, there are hundreds of different biocatalytic processes that are involved in various pharmaceutical, chemical, food, and agro-indusries. Biocatalytic processes are similar in many ways to conventional processes and the key factors to be taken into account for both single and multi-step reactions are reaction kinetics and stability. The biocatytic process begins with the recognition of target reactions, biocatayts discovery, analysis, engineering and chemical process modelling.[2]

Biocatalysts have many advantages over chemocatalysts as they are very proficient catalyst for a wide variety of chemical reactions, they are biodegradable, are innocuous if

used correctly, low consumption of energy because mild conditions are required, less by-products are produced, large scale preparation is possible (i.e. industrial application).[3]

Biocatalysis will have a significant effect in future: the enhanced potential to use enzymes to catalyse chemical reactions in industrial processes, drug substances processing. Flavours, fragrances, organic substances and polymers- chemicals that really affect every aspect of our life. If we implement biocatalysis as our key chemical processing method, we are going to bring an environmental friendly and less expensive technology.

1.2. Biocatalytic promiscuity:

Biocatalytic promiscuity refers to an enzyme's ability to catalyse an accidental side reaction besides its primary function.

Indeed, it is believed that all enzymes have evolved due to promiscuous activities in primitive generalist enzymes[3]. The enhanced selectivity and specificity of catalysts is deemed to be the result of evolution and divergence [4][5][6][7][8]. Divergent evolution is believed to start with duplication of gene [9]. The duplicated gene is now able to evolve promiscuous activity. Enzyme Promiscuity usually doesn't impact an organism, if it is not affecting the native activity rate, and if the promiscuous reaction substrate is not natural to the enzyme.[3] Promiscuous property is usually concealed under indigenous catalytic transformation and is only noticeable under certain conditions, which makes it hard to discover if not deliberately sought for[7][10][11].

Enzyme promiscuity is generally acknowledged as an ultimately beneficial aspect for the new enzyme evolution. It helps an organism to live in an altered environment. In fact, the promiscuous catalytic ability of enzymes develops via evolution. In nature, the specificity of the enzymes tends to improve in order to just perform function that can satisfy the cells[12]. Natural selection produces enzymes which are adaptable to the environment and can quickly evolve as a result of environmental changes[13]. Nature has used common binding sites and reaction mechanisms in order to increase the number of chemical transformations. This has contributed to a variety of enzyme superfamilies[14]. Enzymes within superfamilies have evolved from primitive ones (i.e. having common ancestors) with minimal modifications in the structure [15][16][17]. Research has shown

that the roles of enzymes may often be related when they share a common ancestor[18]. Furthermore, this information helps biotechnologists to broaden enzyme applications into a wide range of industrial applications to build versatile green, chemical synthesis tool[19][20][21][22]. There are many enzymes which showed catalytic promiscuous behaviour towards a variety of reactions depending on the reaction condition for eg. Lipase in addition to its esterase property, it is also effective in aldol, transesterification, Michael addition reaction; phosphatase can also act as sulfatase as they are closely linked and many other examples involving enzymes like aminoacyclase, monooxygenase, glutathione S-transferase, chymotrypsin etc.[22]

Although, most broad varieties of substrate promiscuity have been shown by native and engineered metalloenzymes, specifically by cytochrome P450 family[22]. Frances H. Arnold **(** Noble prize winner-2018 for" directed evolution of gene") described how just a few mutations in amino acid sequence in enzymes can tune the function and they are able to catalyse wide variety of chemical reactions[18]. In last two decades, new biocatalysts generated by directed evolution of heme proteins have been used to catalyse myriad of chemical reactions, namely- C-C coupling, C-B, C-Si bond formation, ring contractions and expansions, sulfoxidation, nitrogen oxidation, epoxidation, decarbonylation, nitration and many more [23][24][25][26].

More interestingly, this promiscuous property is observed in proteins like serum albumins[27][28][29]. Serum albumins can bind and catalyse proton transfer catalysis i.e. Kemp elimination (KE) reaction with remarkably high efficiency and "accidental specificity", also serum albumins have shown catalytic ability for asymmetric oxidation, reduction, cycloaddition among many others in different solvents like ionic liquids and organic media.

Aldoxime dehydratase is also known for showing promiscuous behaviour towards Kemp elimination reaction. Its main function is to remove H_2O from aldoxime (substrate) by abstracting the β proton of aldoxime by distal histidine (Figure 1(b)). Similarly, it can catalyse non-natural Kemp elimination reaction where the distal histidine (acts as base) of this enzyme abstracts proton from 5-nitrobenzisoxazole (Kemp elimination substrate), leads to the formation of cyanophenol (Kemp elimination product) and the transition state is stabilised by its heme environment[30].

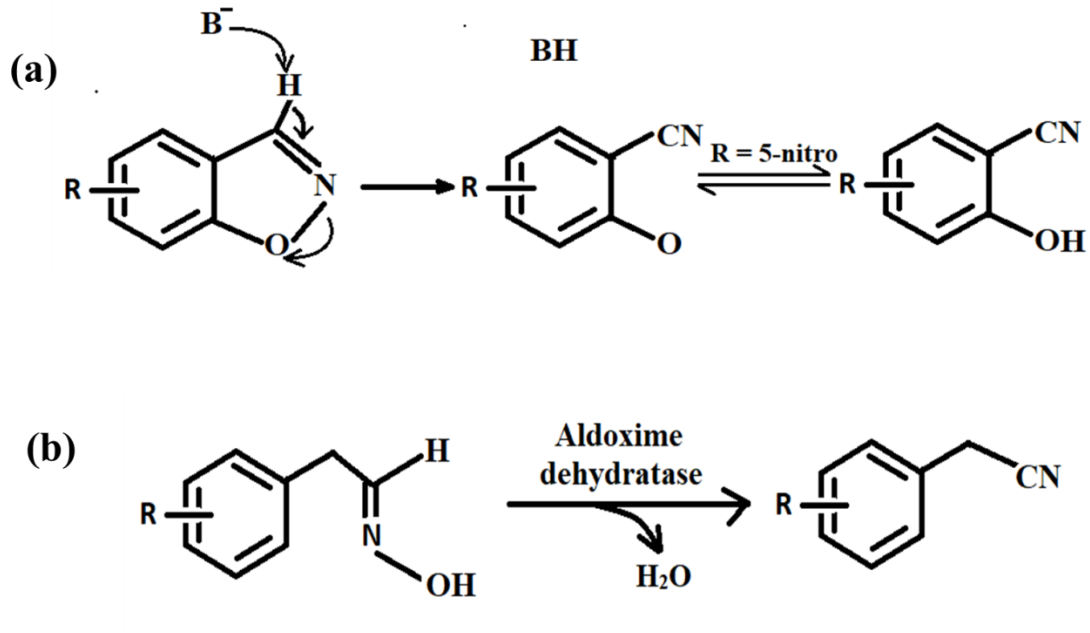

Figure 1: Schematic representation of (a) Base catalysed Kemp elimination reaction (b) Dehydration of aldoxime catalysed by aldoxime dehydratase.

1.3 Cytochrome C:

It was first discovered by Charles A. MacMunnin in 1886, and David Keilin re-discovered it again in 1925 and also identified its role in cell respiration. It is small globular heme protein having molecular weight ~12500. It is highly soluble in water. It is most omnipresent early earth protein which is present in all aerobic organisms as well as in some anaerobic organisms[31][32]. Yamanaka et al. delineated phylogenetic tree by correlating the primary amino acid sequence of cyt c (from different species ranging from microbial algae to mammalian cell), structure of the heme part and their reactivity towards cytochrome c oxidase[31]. In 1976, Jensen suggested that primitive enzymes/proteins possess broad substrate specificity (hence can perform many function in addition to their primary function) in contrast to lately developed enzymes/ proteins in evolutionary process [4].

1.3.1. Sequence and functions of cytochrome c:

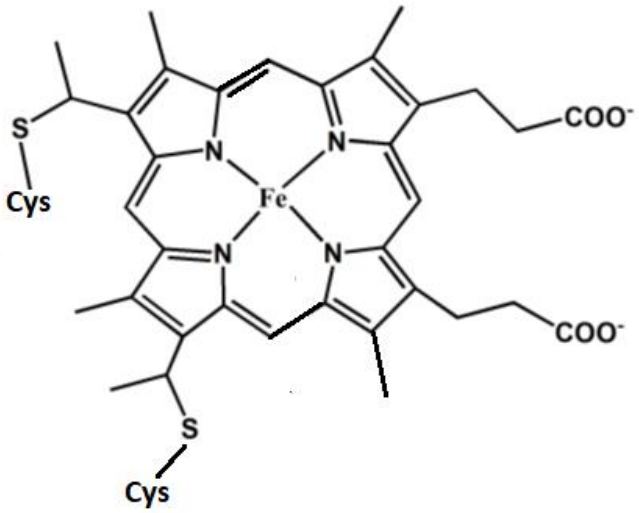

Figure 2: Structure of heme.

1.3.1.1. Cyt c amino acid sequence:

Acetyl.Gly.Ap.Val.Glu.Lys.Lys.Ileu.Phe.Val.GluNH_2Lys.**CyS.Ala.Glu.NH_2CyS.**His.Thr.Val.Glu.Lys.Gly.Gly.

HEME

Lys.His.Lys.Thr.Gly.Pro.Asp.NH_2.Leu.His.Gly.LeuPhe.Gly.Arg.Lys.Thr.Gly.Glu. NH_2.Als.Pro.Gly.Phe.Thr.

Tyr.Thr.Asp.Ala.Asp. NH_2 Lys.Asp. NH_2 Lys.Asp. NH_2.Lys.Gly.Ileu.Thr.Try.Lys.Glu.Glu.Thr.Leu.Met.Glu.

Tyr.Leu.Glu.Tyr.Leu.Glu.Asp. $NH_2$2Pro.Lys.Lys.Tyr.Ilue.Pro.Gly.Thr.Lys.Met.Ilue.Phe.Als.Gly.Ilue.Lys.Lys.

Lys.Thr.Glu.Arg.Glu.Asp.Leu.Ilue.Ala.Tyr.Leu.Lys.Lys.Ala.Thr.Asp. NH_2.Glu.COOH

1.3.1.2. Functions of cyt c:

It is found in the compartment between inner and outer mitochondrial membrane where it shuttles electron between complex III and complex IV of respiratory chain[33][34].

Apart from the primary function of cyt c as electron transporter, it is known for peroxidase activity in lipid membrane where it exposed its heme moiety by opening up the tertiary structure[35][36].

1.4 Investigation of Kemp elimination Reaction:

1.4.1 Kemp Elimination:

It involves proton abstraction from Carbon of a benzisoxazole ring which leads to the opening of the benzisoxazole ring and results into the formation of cyanophenol product. Kemp elimination of 5-nitrobenzisoxazole (5-NBI) results in the formation of 2-cyanophenol (2-CNP) product [37].

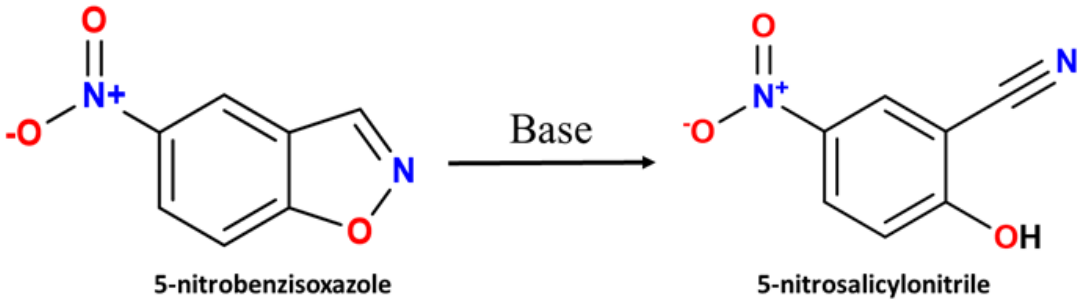

Figure 3: Representation of acid-base type catalysis, kemp elimination.

It is highly exothermic, irreversible and follows concerted E2 mechanism[28]. Rate of the reaction is determined by the concentration of base. Only Carbon-3 proton is involved during the abstraction of proton by base. Organic solvents like dimethylsulfoxide (DMSO) are known to accelerate this reaction [38][37].

The reaction occurs at the stern layer i.e. interface between water and micellar head. Cationic micelles are known to accelerate the rate of reaction because positively charged micelles can stabilize the negatively charged transition state [37].

Kemp elimination is important in understanding metabolism of various isoxazole based therapeutic drugs, like – leflunomide (anti inflammatory drugs), zonisamide (treatment of epilepsy and parkinsons disease) as these drugs undergo KE during their metabolism.

1.4.2 Albumins catalysed KE:

Albumins are globular, non-glycosylated and most abounding protein found in the blood of mammals. They are highly soluble in water and contain a hydrophobic pocket in their structure[27]. Albumins show proton transfer catalysis accidentally with high specificity. Although true catalytic site is absent in BSA and HSA yet they are able to show proton transfer catalysis. Presence of Lysine moiety lys-222 and lys-199 in BSA (Bovine Serum Albumin) and Human Serum Albumin (HSA) respectively are responsible for this catalysis, because these sites are basic in nature and hence responsible for the abstraction of proton i.e. lysine moiety acts as base and therefore leads to the kemp elimination product[29].

Serum albumin shows promiscuous properties firstly it can bind and catalyse proton transfer and secondly, it shows catalytic ability for asymmetric oxidation, reduction, cycloaddition among many others in different solvents like ionic liquid organic media.

1.4.3 Cyt C catalysed kemp elimination:

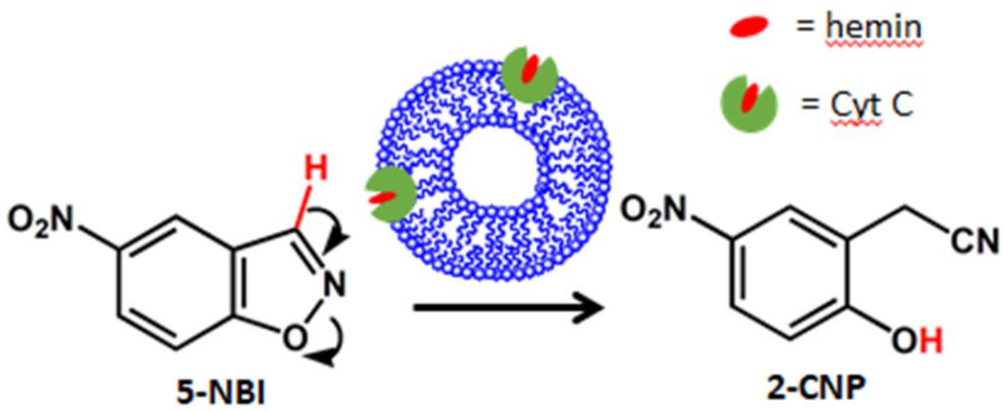

Figure 4: Schematic representation of the kemp elimination (KE) reaction catalysed by cytochrome c (cyt c) bound in vesicles.

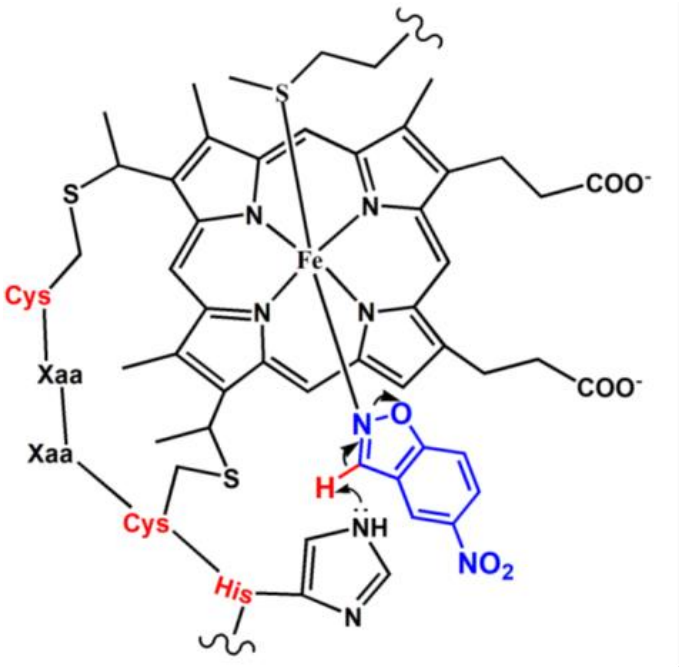

Figure 5: Schematic representation of the heme co-ordination of the substrate (NBI) which subsequently resulted histidine (His-18) catalysed proton transfer.

Motivation behind investigating KE by cyt is that it is largely believed that more primitive protein can perform multiple functions, and cyt c is one such protein which is most primitive and omnipresent protein that can perform multiple functions which made us curious to investigate detailed study of proton transfer catalysis by cyt c. Fortunately we have found that cyt c is able to show proton transfer catalysis but the effect is strictly restricted to self-organized system (like micelles and vesicle) or membrane mimetic media. Further investigation with various different enzymes/ proteins like haemoglobin, lysozyme, catalase, HRP, Horseradish Peroxidase (HRP), Lipase, Lysozyme, Alkaline Phosphatase, Catalase has also been carried out but none of these have been found to show any positive results.

Chapter 2

Experimental Setup and Methods

This chapter describes experimental techniques and procedures involved to study the proton transfer catalysis of 5-nitrobenzisoxazole (NBI) by cytochrome c and various heme proteins / enzymes.

2.1 Experimental Methods:

2.1.1 UV-Vis Spectroscopy:

UV-Vis studies were performed using Varian Cary 60 (Agilent technologies) spectrophotometer. The proton transfer catalysis was carried out by following the product formation at 380 nm. Total reaction volume in the cuvette was fixed at 1 ml and cuvette of path length 1 cm was used for the entire kinetic study. All measurements have been performed at 25 ^{o}C.

2.1.2 Fluorescence Spectroscopy:

Fluorescence measurements were performed using SHIMADZU Model RF-6000 Spectrofluorophotometer.

2.1.3 Nuclear magnetic resonance spectroscopy:

The NMR spectra were recorded in Bruker Avance-III 400 MHz spectrometer. ^{1}H and ^{13}C NMR were recorded at operation frequencies 400 MHz and 100 MHz, respectively. $CDCl_3$ and DMSO-d6 were used as the solvents and tetramethylsilane (TMS) as the internal standard for recording the samples. The chemical shift values are reported as delta (δ) units in parts per million (ppm).

2.1.4 Mass Spectroscopy:

High resolution mass spectra have been recorded using Waters Synapt G2-Si Q-TOF mass spectrometer in Electrospray ionization (ESI) mode.

2.1.5 Optical and Fluorescent microscopy:

The optical and fluorescence microscopic images were collected using Olympus total internal reflection fluorescence microscope (IX83 P2ZF inverted microscope equipped with IX83 MITICO TIRF illuminator).

2.1.6 Transmission Electron Microscopy:

The Transmission Electron Microscopy images were taken on JEOL JEM-F200 microscope. Staining of the vesicle was done using 1% phosphomolybdic acid solution.

2.1.7 Dynamic Light Scattering:

The Dynamic Light Scattering (DLS) data was recorded on Malvern Zetasizer Nano-ZS90.

2.1.8 Circular dichroism:

Circular dichroism (CD) measurements were carried out on a Characin spectrophotometer (Applied Photophysics) using a 1 mm path length quartz cell. The concentration of cytochrome c used for the CD measurement was 20 µM. The spectra were recorded with a scan range of 200-550 nm. All measurements were recorded in triplicate.

2.2 Experimental Procedure:

2.2.1. Synthesis of 5-nitrobenzisoxazole:

It has been synthesized as reported in literature[39]. 0.5 g of 1,2-Benzisoxazole was dissolved in 5 ml conc. sulphuric acid at room temperature. Then, 0.5 ml of a mixture of conc. nitric acid (0.6ml) and conc. sulphuric acid (0.2 ml) was added slowly to the above solution and then stirred for 30 min at room temperature. The solution was then poured into a 20 ml ice-water mixture and was stirred and thawed for 10 min. The white precipitate obtained was filtered, washed with cold ethanol and the solvent was dried under a high vacuum. The product was recrystallized in abs. ethanol to obtain a white, crystalline solid.

2.2.2. Synthesis of 2-cyano-4-nitrophenol:

It has been synthesized as reported in literature[39]. To a solution of 0.1 g of 5-nitrobenzisoxazole in 2 ml ethanol and 1 ml water, 3 ml of 2M NaOH was added and the mixture was allowed to stand for 10 min. During this time, HCl was added slowly to bring the pH of the mixture to 1. The solution was extracted with dichloromethane and the solvent was evaporated under vacuum. The product was air-dried to obtain a light yellow coloured solid. Yield: 66.78%.

2.2.3 Preparation of CTAB-SDS catanionic vesicles, DOPC and AOT vesicles:

2.2.3.1 CTAB-SDS catanionic vesicles:

Preparation was based on a previously reported procedure[40] [41][42]. Stock solutions of CTAB (10 mM) and SDS (30 mM) prepared in buffer were mixed as such to give a final concentration of 2 mM CTAB and 10 mM SDS in the solution, forming CTAB-SDS catanionic vesicles[42].

2.2.3.2 DOPC and AOT vesicles:

Preparation was based on a previously reported literature [43] [44]. 1mL chloroform was added to 3.3 mg 1,2-dioleoyl-sn-glycero-3-phosphocholine (DOPC) in a 2 mL vial and then transferred to a 25 mL round-bottomed flask. To get the film at the bottom of the RB, the above solution was evaporated under vacuum for around 30 min at 30 ^{o}C. Then, 5 mM phosphate buffer was sonicated for 1 hr at room temperature to get a de-oxygenated buffer and 2 mL of this buffer was then added to DOPC film obtained above. A small bead was added to the RB and then by providing the N_2 environment, it was stirred using magnetic stirrer for 2 hrs. at 1100 rpm. A milky and homogeneous solution was obtained and it was stored at 4 $^{\circ}$C until needed.

AOT vesicles were prepared in a similar manner as described above.

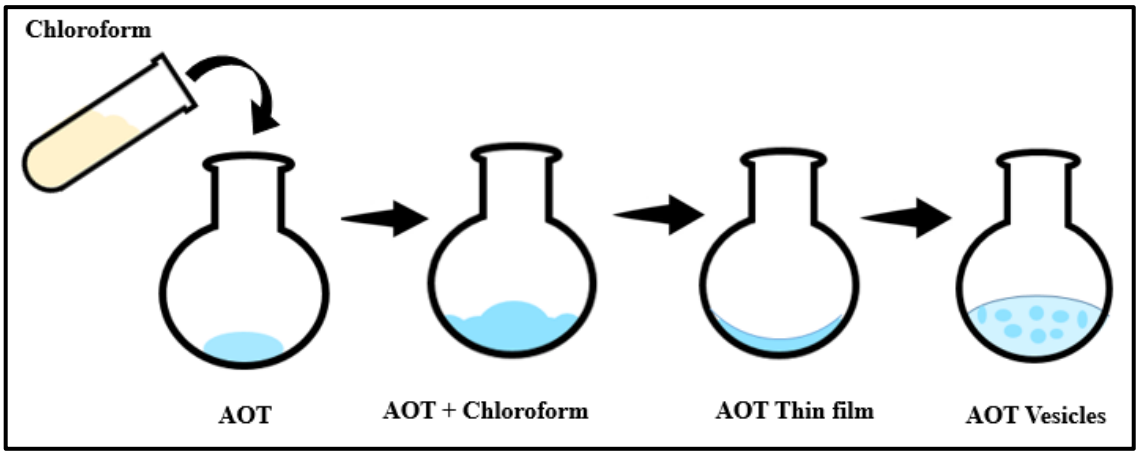

Figure 6: Formation of AOT Vesicles

2.2.4. Demetallation of Hemin:

Demetallation was based on a previously reported procedure [45]. 5mL concentrated hydrochloric acid was added to 0.6 mL acetic anhydride at 5°C. Fe(III) DH (0.08 mmol) and ferrous sulphate (0.315 mmol) was added to it, after that it was transferred to ultrasonic bath having frequency 40kHz then the solution was irradiated by ultrasonic waves for 1hour. The Brown precipitate obtained was filtered and washed with distilled water. It was washed and filtered three times, then it was recrystallized by hot acetone and vacuum dried at 100 $^{\circ}$C for 3 hrs. to get pure solid product.

2.2.5 Preparation of BSA -FITC and CYT c-FITC:

Cyt c-FITC has been prepared in a similar manner as BSA-FITC, which is reported in literature[46]. 2 mg/mL cyt c solution was dissolved in sodium carbonate buffer (pH= 9) at room temperature. Then FITC (1mg/ml) was dissolved in DMSO (fresh FITC solution has been used always). This solution was wrapped in aluminium foil to protect it from light. 200 µL FITC solution was slowly added to the cyt c solution and covered with aluminium foil and kept at 4°C for 5 hrs. The reaction was quenched by ammonium chloride solution (final concentration of it kept at 50 mM). The vial was kept at 4 °C for 2 hrs. The above prepared conjugation was then purified by gel filtration (Sephadex G-25), using 5mM phosphate buffer (pH 8).

UV scan spectra of fractions obtained above were taken and it was observed that cyt c-FITC showed peaks for cyt c and FITC at 410 nm and 495 nm respectively (as shown in figure 7). In both the cases, tagging efficiency was almost 1:1.6 (protein:dye).

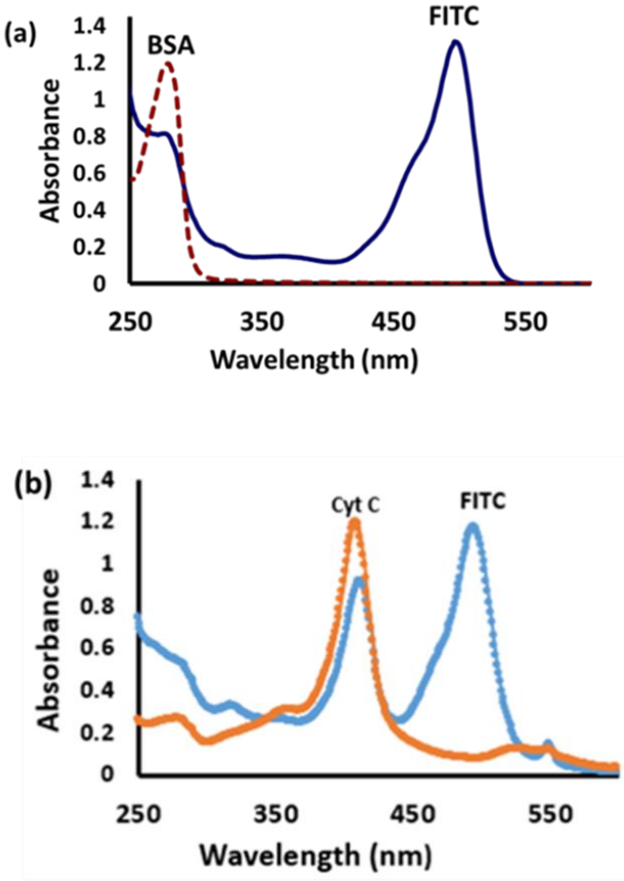

Figure 7: UV-vis spectra of (a) FITC-BSA, and (b) FITC-cyt c.

2.2.6 Preparation of Apo-Cytochrome C

Apo-cyt c has been prepared as reported in literature[47]. Ag_2SO_4 silver sulphate (8 mg in 900 µL water) and 80 µL of acetic acid were added to 4.8 mg cytochrome c solution in 100 µL of water. The above-prepared solution was kept for incubation at 40°C for 4 hrs. Then it was centrifuged to remove heme aggregates. The obtained solution was purified using Sephadex G-25 column equilibrated with 0.1N acetic acid. The protein was eluted by 5 mM phosphate buffer (pH=8). Fractions of 500 µL were collected and their UV scan spectra were taken. It was observed that in the case of apo-cytochrome c, 410 nm peak was missing which was present in cytochrome c (Figure 8). Also tryptophan fluorescence retained as quenching effect of hemin moiety is no longer there (Figure 32(d)). In SDS micelle, there is a blue-shifting of the tryptophan fluorescence due to hydrophobic micellar environment.

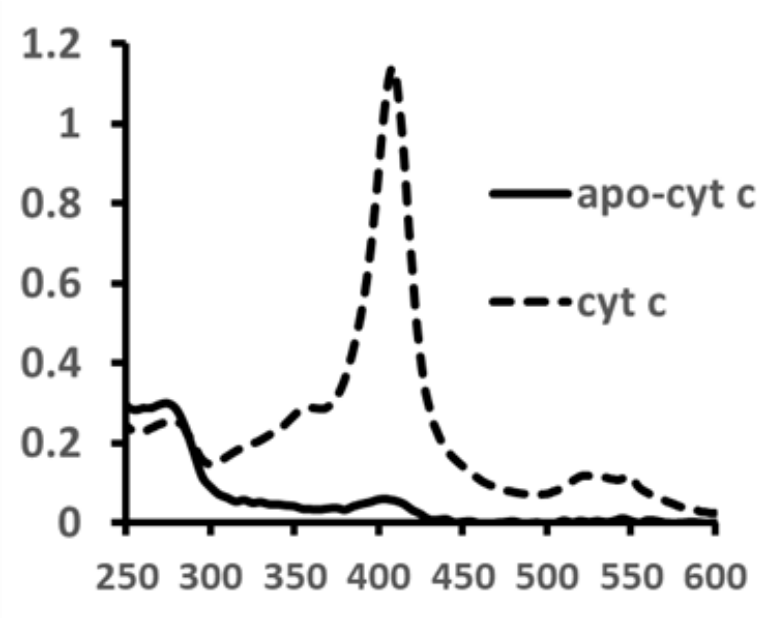

Figure 8: UV-vis spectra of apo-cyt c and cyt c to show the disappearance of soret peak (at 405 nm) due to removal of hemin moiety.

Chapter 3

Results and Discussions

3.1 Characterization of substrate and product:

At first the KE substrate, 5-nitrobenzisoxazole (NBI) which in presence of base converted to 2-cyanophenol (2-CNP), was synthesised and characterized (as shown in figure 9 and figure 10).

3.1.1 Characterization of substrate (5-NBI):

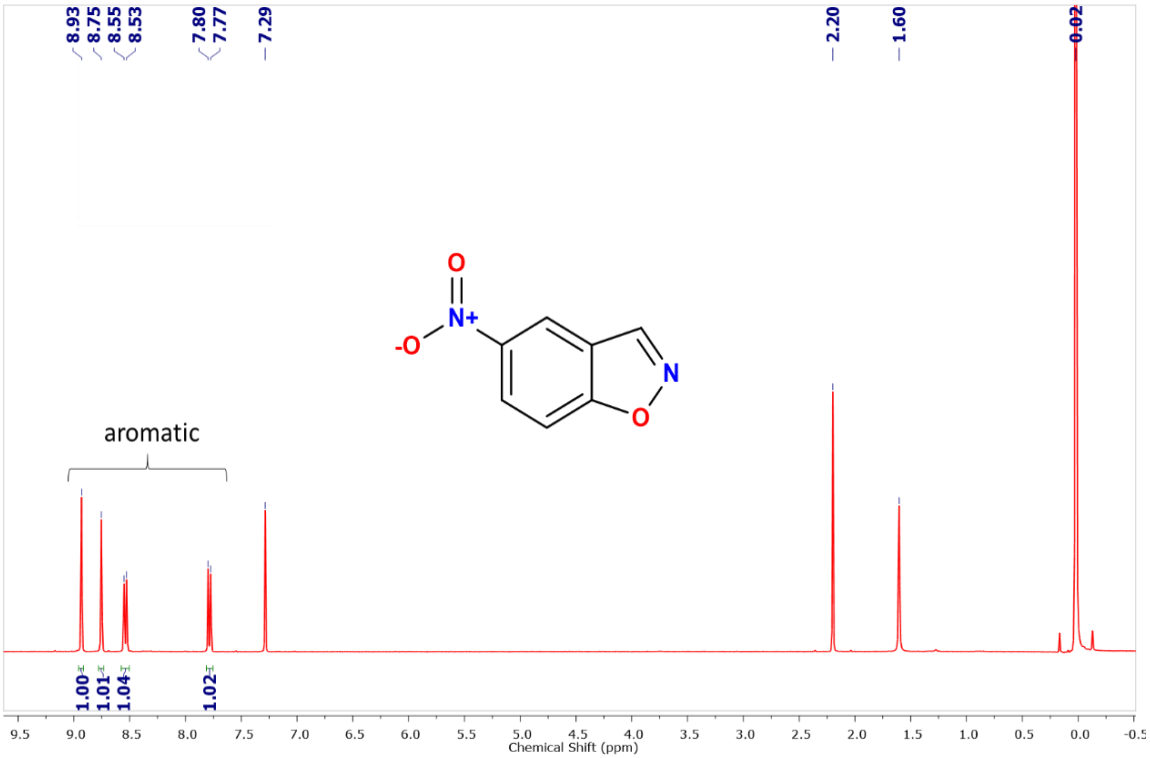

^{1}H NMR (400MHz, $CDCl_3$): δ 7.79 (d, 1H), 8.54 (d, 1H), 8.75 (s, 1H), 8.93 (s, 1H). ^{13}CNMR (100MHz, $CDCl_3$): δ 164.39, 147.06, 141.05 125.64, 121.87, 119.24, 110.52. 6

Figure 9: ^{1}H-NMR spectrum of 5-nitrobenzisoxazole (NBI).

3.1.2 Characterization of Product:

^{1}H NMR (400MHz, DMSO-d6): δ 7.17 (d, 1H), 8.36 (d, 1H), 8.61 (s, 1H)

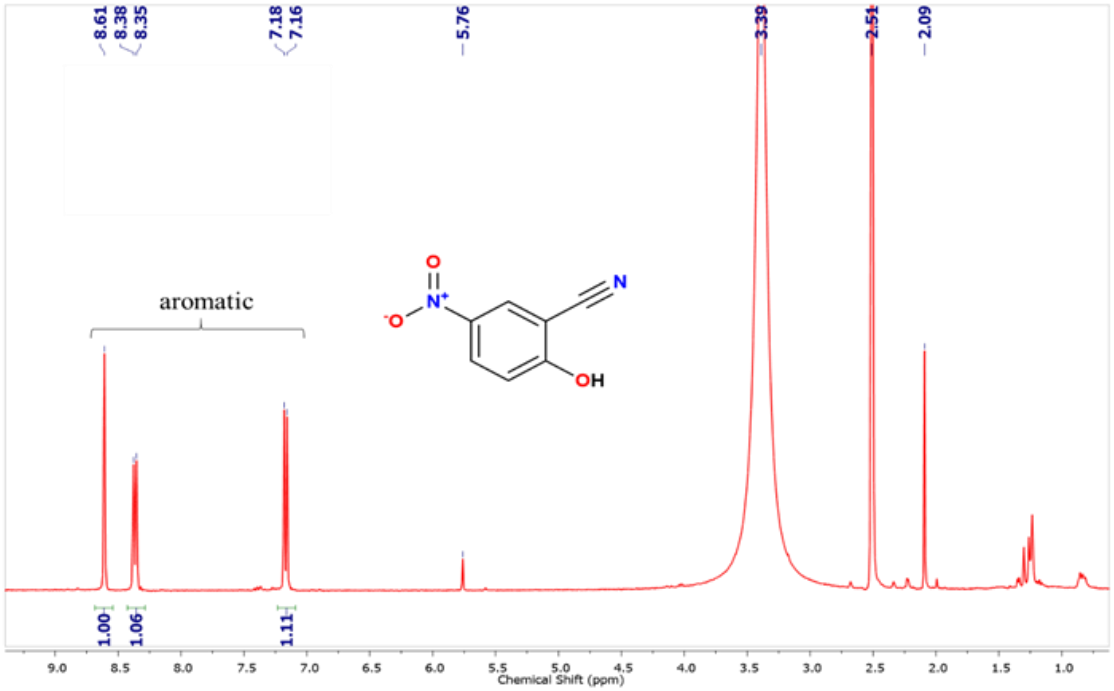

Figure 10: ^{1}HNMR spectrum of 2-cyano-4-nitrophenol (2-CNP).

3.2 UV-Vis spectra of NBI (substrate) and 2-CNP (product):

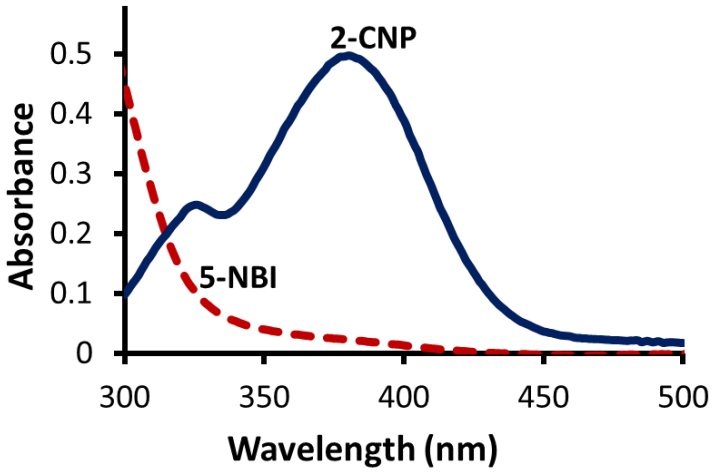

Figure 11: UV-Vis spectra of NBI and 2-CNP.

3.3 Molar Extinction coefficient of product in different system:

Molar extinction coefficient of separately synthesized 2-CNP was also checked at each media used in this study for accurate calculation of the concentration.

Table 1: Molar Extinction coefficient (at λ = 380 nm) of the product 2-CNP in different system.

System	Molar Extinction Coefficient ($M^{-1}cm^{-1}$) at 380 nm
Buffer (pH=6.0)	**15640**
Buffer (pH=6.8)	**15780**
Buffer (pH=7.4)	**16000**
Buffer (pH=8.0)	**16240**
5 mM SDS (pH 8.0)	**16400**
10 mM SDS (pH 6.0)	**15800**
10 mM SDS (pH 6.8)	**16050**
10 mM SDS (pH 7.4)	**16400**
10 mM SDS (pH 8.0)	**16770**
1mM CTAB (pH 8.0)	**16400**
0.5 mM CTAB (pH 8.0)	**16200**
2 mM CTAB + 10 mM SDS (pH 6.0)	**15690**
2 mM CTAB + 10 mM SDS (pH 6.8)	**15810**
2 mM CTAB + 10 mM SDS (pH 7.4)	**16100**
2 mM CTAB + 10 mM SDS (pH 8.0)	**16200**
AOT (pH 8.0)	**15900**
DOPC (pH 8.0)	**15700**

3.4 Kemp Elimination catalysis activity of BSA and Cyt c in different systems:

3.4.1 BSA in Buffer:

In the beginning, already known KE catalytic activity of BSA was verified in the 5mM phosphate buffer at pH8 (mostly used buffer in this study). The k_{cat} and K_M values of BSA towards KE catalysis of NBI were found to be 9.2 ± 1 min^{-1} and 154 ± 16 µM respectively (Table 3).

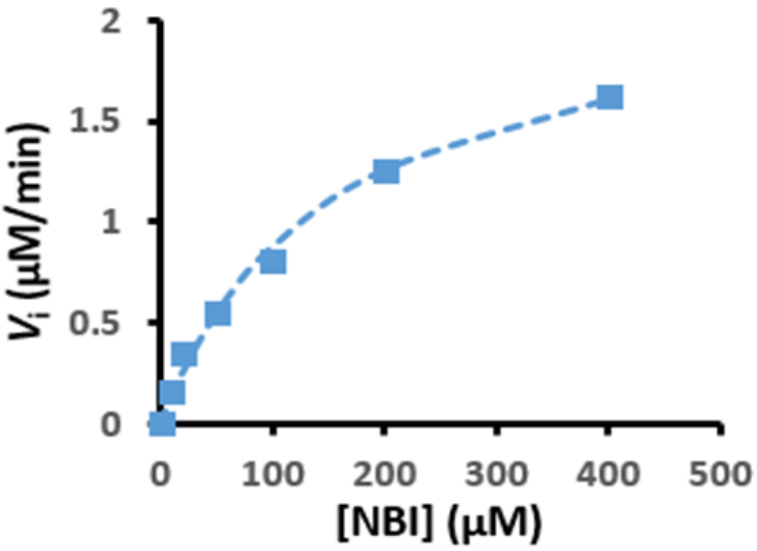

Figure 12: V_i of KE catalysis in presence of BSA (0.25 µM) at varying NBI concentration in phosphate buffer (pH 8, 5 mM). The dotted lines are the data fit according to a Michaelis–Menten mechanism.

3.4.2. Cyt c in Buffer:

As our main aim was to understand KE catalytic activity of cyt c, therefore it was studied in the same buffer (5mM Phosphate buffer (pH = 8)) as used in the case of BSA by changing the concentration of both cyt c (1-10 µM) as well as substrate (0-500 µM) but in none of the cases it showed any catalytic effect (shown in fig 13.). Hence this clearly indicates that, unlike BSA cyt c does not contain any hydrophobic pocket in its structure to catalyse proton transfer KE catalysis.

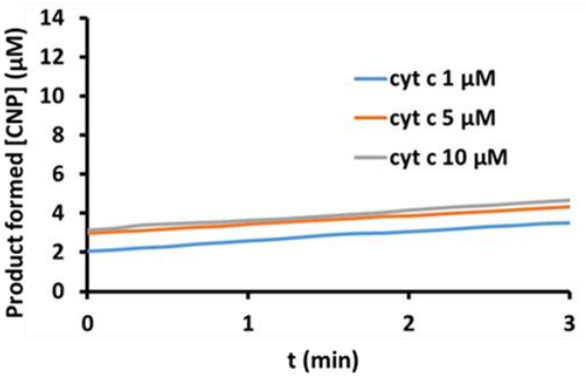

Figure 13: Representative plot for product formation as a function of time for different concentrations of cyt c at fixed substrate (NBI) concentration in phosphate buffer (pH 8, 5 mM).

Table 2: Initial rate of formation of product at different concentrations of cyt c in phosphate buffer (pH 8.0, 5 mM)

cyt c conc. (µM)	Vi (µM/min.)
0	**0.15 ± 0.02**
1	**0.17 ± 0.03**
5	**0.17 ± 0.04**
10	**0.2 ± 0.03**

3.4.3 Cyt c in Self-organised systems:

Apart from its primary function as electron transporter in respiratory chain, cyt c is also known for its peroxidase like property, only when it comes in contact with membranes like micelles, vesicles, reverse micelles (i.e. in self organised media) and gets bound to them, by doing so it gets unfolded and can expose its heme moiety[34][35]. Now this permits the peroxide substrate to bind with iron centre to show its peroxidase property. This made us curious to check its KE catalytic property in different systems like cationic, anionic, zwitterionic micelle, vesicular medium.

3.4.3.1 In SDS anionic micelles:

To check cyt c activity in self organised system, Sodium dodecyl sulphate (SDS) was used as anionic surfactant system, it was found that in absence of cyt c, at fixed substrate concentration (NBI= [100µM]) and at different SDS concentrations (0.1-30mM) has not shown any KE catalytic effect (fig. 14).

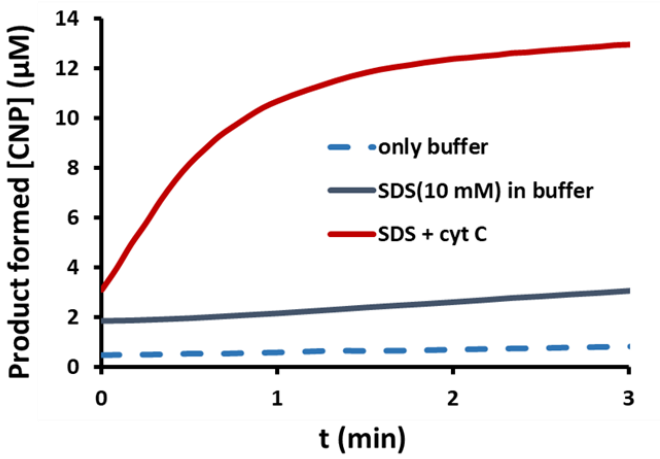

Figure 14: Representative plot for product formation as a function of time in only buffer, SDS micelles (10 mM) in absence and presence of cyt c (5 µM) at fixed substrate (NBI) concentration (100 µM) in phosphate buffer (pH 8, 5 mM).

After that the KE catalytic activity was carried out in presence of cyt c under similar reaction conditions. It was observed that the initial rate (V_i) started to increase at SDS = [5mM] and it reached maxima at SDS = [10-15mM] above that concentration the rate started to gradually decline (as shown in figure 15). The maximum catalytic rate obtained was 16±1µM and this is 90 times higher than uncatalyzed rate in buffer. These results shows that once micelles of SDS are formed (CMC of SDS in our experimental condition was obtained around 6mM) cyt c started to show higher catalytic activity.

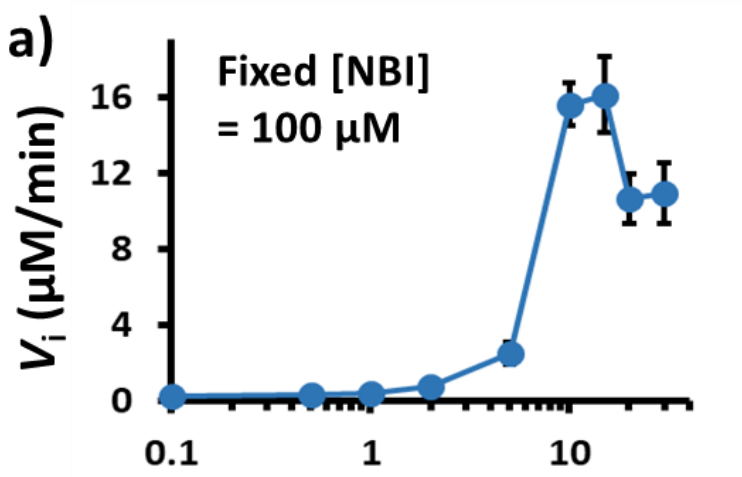

Figure 15: Initial rate (Vi) of KE catalysis at fixed substrate concentration (NBI = [100µM]) in presence of cyt c = [5µM] as function of varying SDS concentration (0.1-30mM).

In Figure 16, initial velocity (V_i) of the KE catalysis was plotted with respect to substrate (NBI) concentration at fixed SDS micelle concentration (10 mM) in absence and presence of cyt c (5 µM). Substrate inhibition was observed after 250 µM of NBI in (SDS + cyt c) system, however, almost no or very low activity was observed in absence of cyt c.

In the absence of cyt c i.e. in only SDS (0-30 µM) no KE catalytic effect was observed at fixed [NBI] = 100 µM. It has been found that cyt c in SDS followed Michaelis-Menten behaviour at 0-250µM substrate concentration range with k_{cat} = 4.0±0.3 min^{-1} and K_m = 61± 10µM (Table 3).

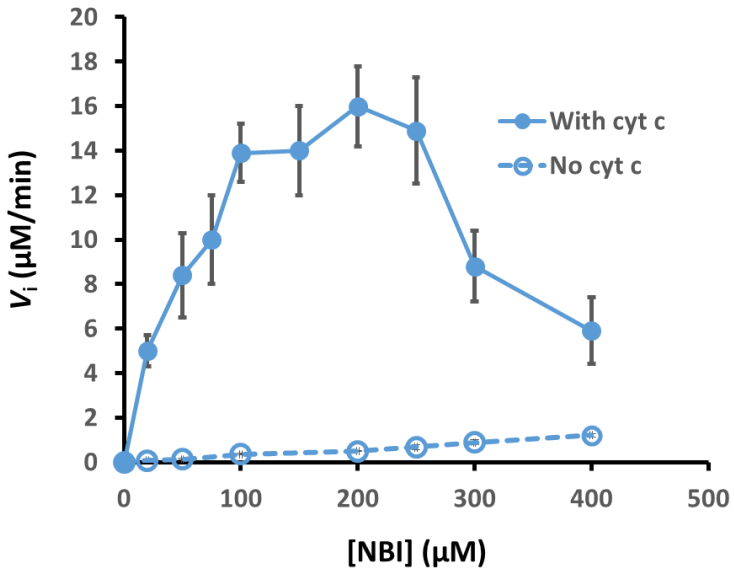

Figure 16: Initial rate (V_i) of KE catalysis in absence and presence of cyt c (5 µM) in SDS micelle (10 mM) at varying NBI concentration (0-400 µM) in phosphate buffer (pH 82, 5 mM).

3.4.3.2 In CTAB cationic micelles:

KE catalysis was then carried out in cetyltrimethylammonium bromide (CTAB) a cationic micellar system. However, cationic micellar environment are known to enhance KE catalysis by stabalizaion of the negatively charged transition state[37][48]. After 0.5mM CTAB started to show strong catalytic activity and it increases to 2mM, after that it started to saturate (CMC of CTAB under our experimental condition was found to be 0.7mM , which is well correlated with this data). Presence of cyt c in CTAB has only increased KE catalytic rate by 1.5 fold.

Figure 17(b) shows that KE catalysis was observed even in absence of cyt c, however, in presence of cyt c (5 µM) the activity is increased by 1.5 fold.

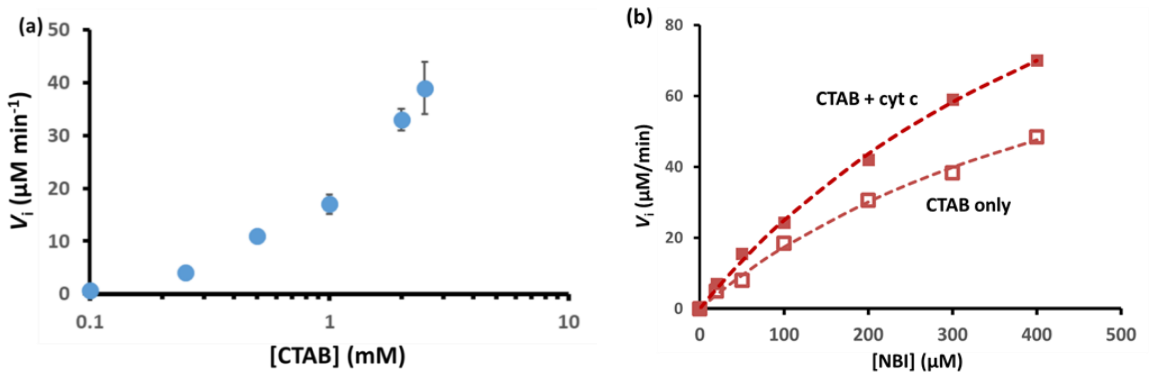

Figure 17: (a) Initial rate of KE catalysis as a function of CTAB concentration at fixed [NBI] = 100 µM in phosphate buffer (pH = 8.0, 5 mM). (b) V_i of KE catalysis at CTAB micelle (1 mM) in absence and presence of cyt c (5 µM) at varying NBI concentration in phosphate buffer (pH 8, 5 mM). The dotted lines are the data fit according to a Michaelis–Menten mechanism.

3.5 KE catalysis effect of gradual SDS addition in CTAB micelles:

It has been observed that presence of SDS diminished KE activity of CTAB micelles and at 10 mM SDS concentration activity of only CTAB micelle almost becomes zero. At 2mM CTAB and 10mM SDS catanionic vesicles were formed which was confirmed by the DLS and TEM (fig.27(c) and 30). In the absence of cyt c in the catanionic vesicles, no catalytic activity was observed at 100 µM NBI but in the presence of cyt c, it showed 250 fold increase in KE rate. The K_{cat} and K_M found in this case was 16 ± 1.0 min^{-1} and 94 ± 6 µM respectively, which is higher than BSA in buffer by 2.6 times considering K_{cat}/K_M (table 3).

9

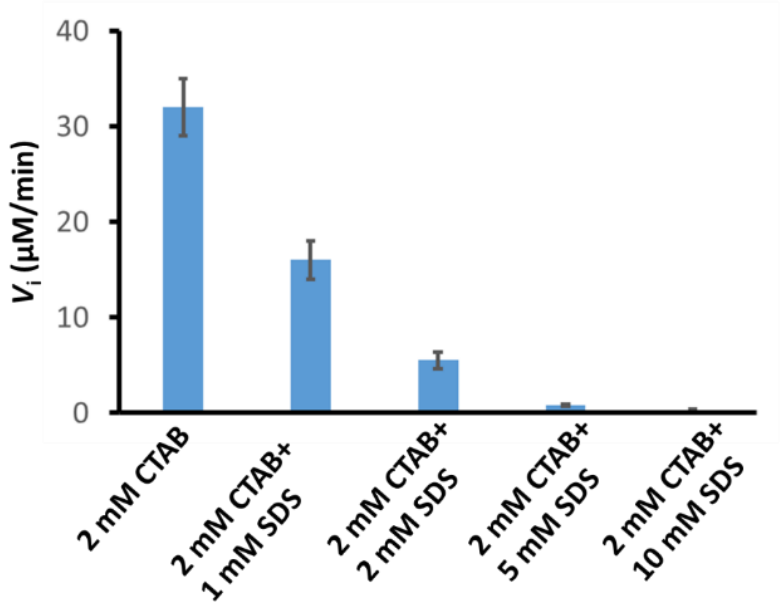

Figure 18: Initial rate (V_i) of product formation in KE catalysis (at fixed [NBI] = 100 µM) with increasing SDS concentration in CTAB solution (2 mM).

Figure 19 shows initial rate of KE catalysis in presence of cyt c in SDS micelles and CTAB-SDS catanionic vesicles.

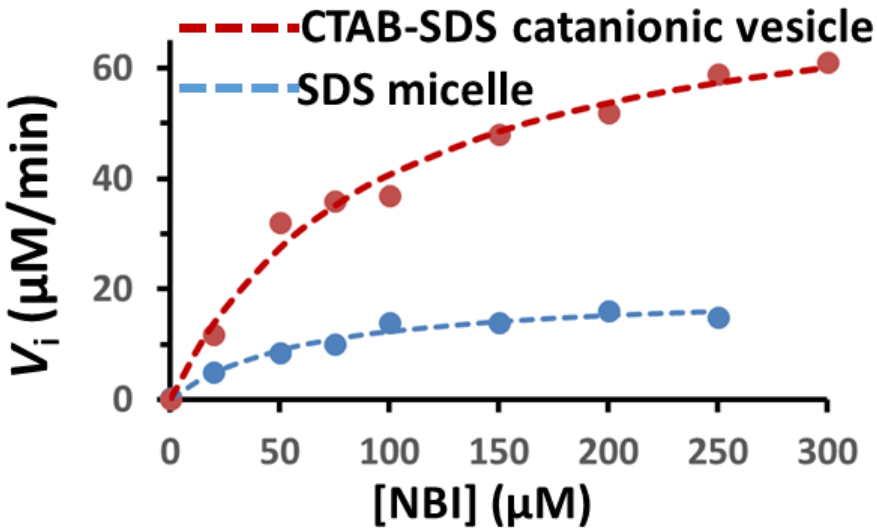

Figure 19: Initial rate (Vi) of KE catalysis in presence of cyt c (5µM) at varying NBI concentration in 10mM SDS and CTAB-SDS catanionic vesicles ([CTAB] = 2mM and [SDS] = 10mM).

3.6 UV scanning kinetics at 30 sec interval in different system:

Cyt c showed the maximum catalytic rate in CTAB-SDS catanionic vesicles than SDS micelles, which is clearly confirmed by the figure 20 (a).

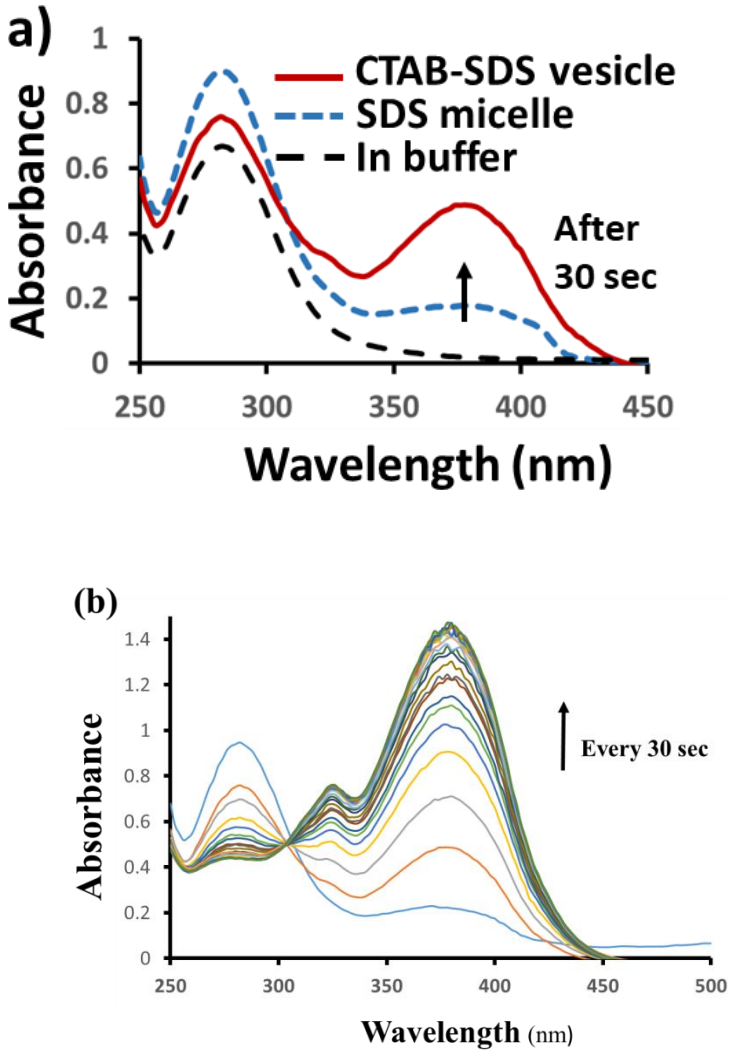

Figure 20: (a) Representative UV-Vis scan spectra taken 30 sec after starting of the reaction at fixed 100µM NBI in presence of 5µM cyt c in buffer, SDS micelle and CTAB-SDS catanionic vesicles. **(b)** Representative UV-Vis scanning kinetics at 30 sec interval after starting the reaction by the addition of 100 µM NBI in presence of cyt c (5 µM) in CTAB-SDS catanionic vesicle. Experimental condition: [CTAB] = 2 mM, [SDS] = 10 mM, phosphate buffer (5 mM, pH 8).

Table 3: Michaelis-Menten constants of different systems (buffer/micelles/vesicles) towards KE catalysis with NBI as substrate in absence and presence of BSA and cyt c. The values in the error bar are standard deviation of triplicate experiments.

	Protein	**V_{max} (μM/min)**	**k_{cat} (min^{-1})**	**K_m (μM)**
Buffer	**BSA (0.25 μM)**	**2.3 ± 0.2**	**9.2 ± 1**	**154 ± 16**
10mM SDS (anionic micelle)	**Cyt c (5 μM)**	**20 ± 1.6**	**4 ± 0.3**	**61 ± 10**
2mM CTAB-10 mM CTAB (catanionic vesicle)	**Cyt c (5 μM)**	**79 ± 5**	**16 ± 1**	**94 ± 6**
1mM CTAB (cationic micelle)	**-**	**114 ± 10**	**-**	**557 ± 30**
1mM CTAB (cationic micelle)	**Cyt c (5 μM)**	**176 ± 13**	**-**	**606 ± 42**

3.7 Comparative enhancement in initial rate (V_i) due to the presence cyt c in various system:

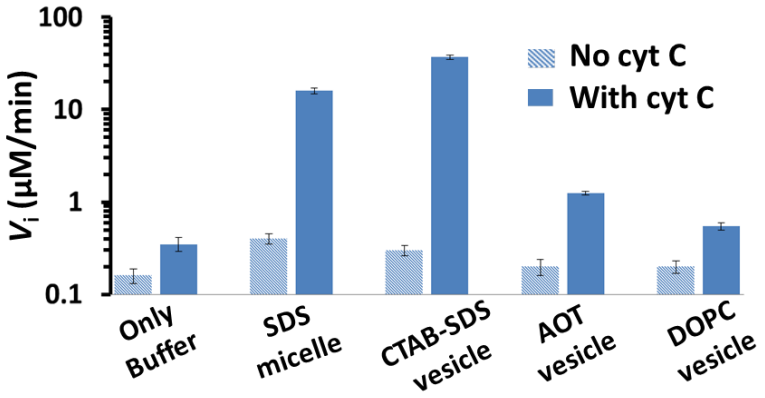

Figure 21: Comparative plot of initial rate (V_i) to show the enhancement effect due to the presence of cyt c in different system.

3.8. CMC Determination of SDS and CTAB:

Critical micellar concentration (CMC) values were determined for CTAB and SDS by using conductometer. CMC of SDS and CTAB were obtained around 5 mM and 0.7 mM, respectively in phosphate buffer (pH 8, 5 mM).

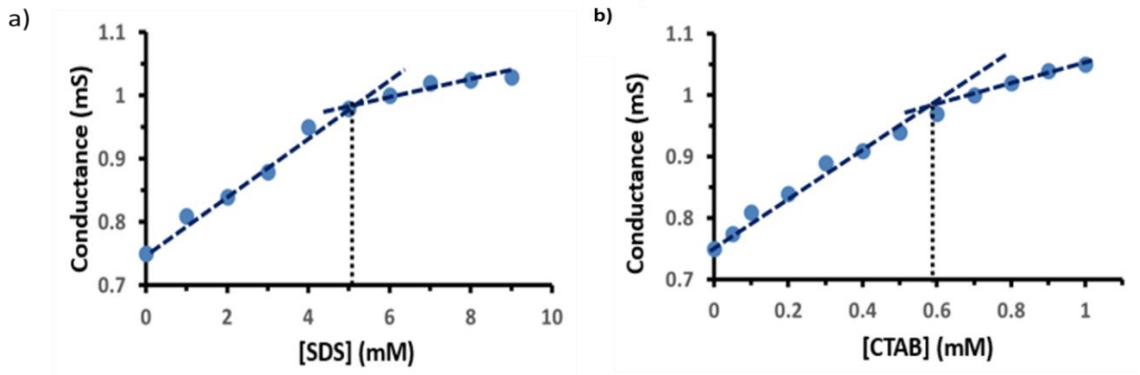

Figure 22: Conductance as a function of a) SDS concentrations and b) CTAB concentrations in aqueous phosphate buffer solution (pH 8, 5 mM).

3.9 Product Inhibition of cyt c in SDS micelles and CTAB-SDS catanionic vesicles:

Competitive type of product inhibition was observed when the product (2-CNP) was added externally in the reaction mixture before the addition of NBI to measure KE catalysis. In case of CTAB-SDS catanionic vesicles, K_i and IC_{50} values were found to be around 0.02 µM and 3.5µM respectively whereas in SDS micelle these values were found to be 0.2µM and IC_{50} ~32µM respectively. Product inhibition effect is much weaker in catanionic vesicles in contrast to SDS micelles, due to high hydrophobic surface area in vesicles than in micelles. It was confirmed by DPH (diphenyl-1, 3, 5-hexatriene) a hydrophobic probe, showed a sharp peak in CTAB-SDS catanionic vesicles than in any other micellar system containing same amount of surfactant (discussed in 3.18)

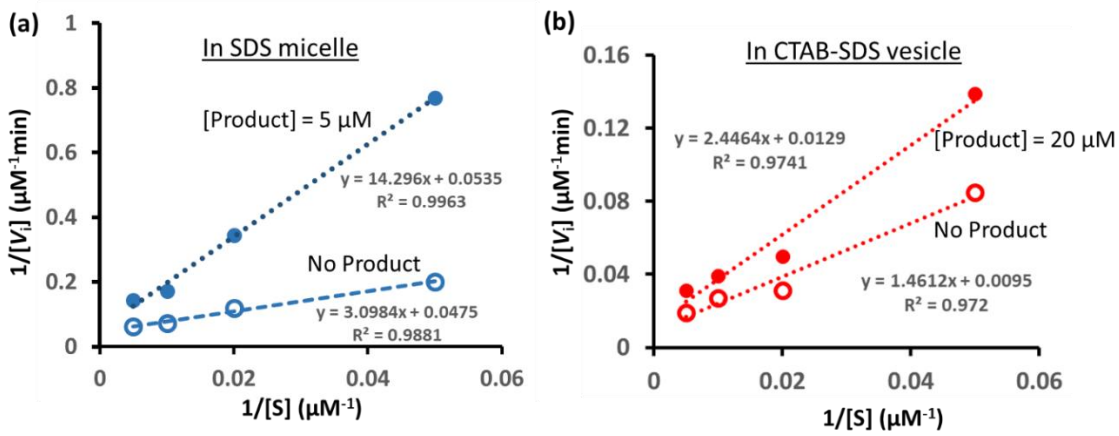

Figure 23: Competitive inhibition illustrated on a double reciprocal Lineweaver-Burk plot ($1/V_i$ in y-axis and 1/[S] in x-axis). A double-reciprocal plot of KE catalysis in the presence and absence of the product (a) in SDS micelle and (b) CTAB-SDS vesicle. Both these plot illustrate that the product (inhibitor) has almost no effect on V_{max} but increases K_M as there are substantial changes in the slope [values of 14.3 (with product), 3.1 (without added product) in SDS micelle and 2.4 (with product), 1.4 (without added product) in CTAB-SDS vesicle] but almost comparable values of the intercept [values of 0.0535 (with product), 0.0475 (without added product) in SDS micelle and 0.0129 (with product), 0.0095 (without added product) in CTAB-SDS vesicle]. These plot suggest that the inhibition type is mostly competitive. [SDS] = 10 mM, [CTAB] = 2 mM, phosphate buffer (pH 8.0, 5 mM)

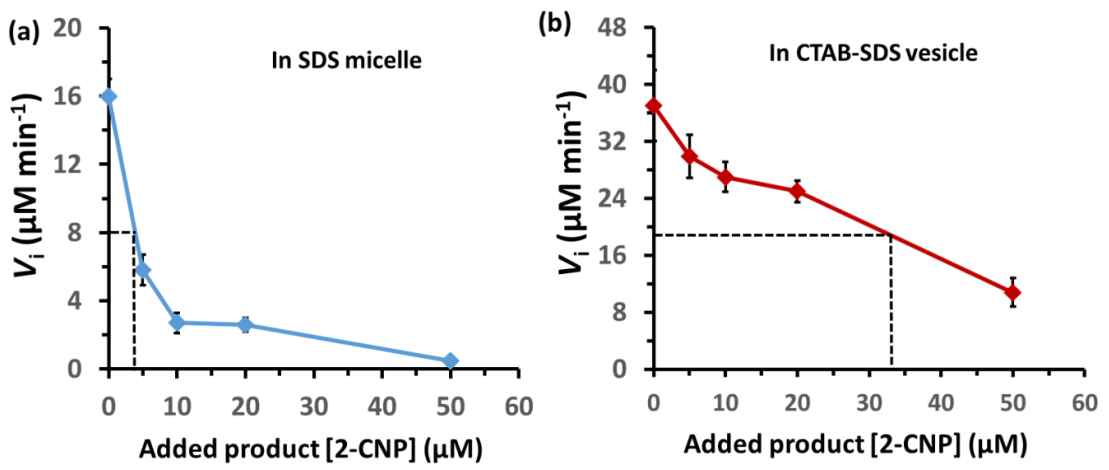

Figure 24: Initial rate of KE catalysis as a function of added product concentration at fixed [NBI] = 100 µM in phosphate buffer (pH = 8.0, 5 mM) measured in (a) SDS micelle and (b) CTAB-SDS vesicle. The dotted line was drawn to show the 50% inhibitory effect (IC_{50}) of the product concentration.

3.10 pH dependent study:

The given plot shows that the reaction rate is almost comparable in pH range 6.8 to 8 and below that it drastically decreased at pH 6 (as shown in figure 25).

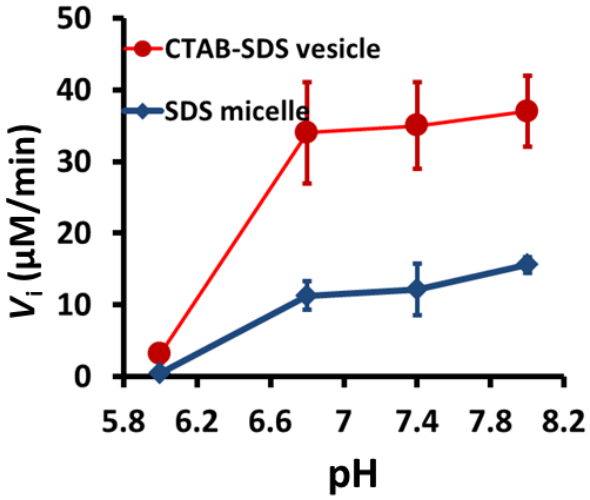

Figure 25: Initial rate V_i of KE catalysis of cyt c (5µM) as a function of pH at fixed NBI concentration (100µM) in SDS micelles and CTAB-SDS vesicles.

3.11 KE catalysis with Hydrogen Peroxide (H_2O_2):

Addition of H_2O_2 reduced the KE catalytic activity, this is probably due to the competition in binding between peroxo group (-OOH) and benzisoxazole moiety with Fe^{3+} of cyt c (figure 26).

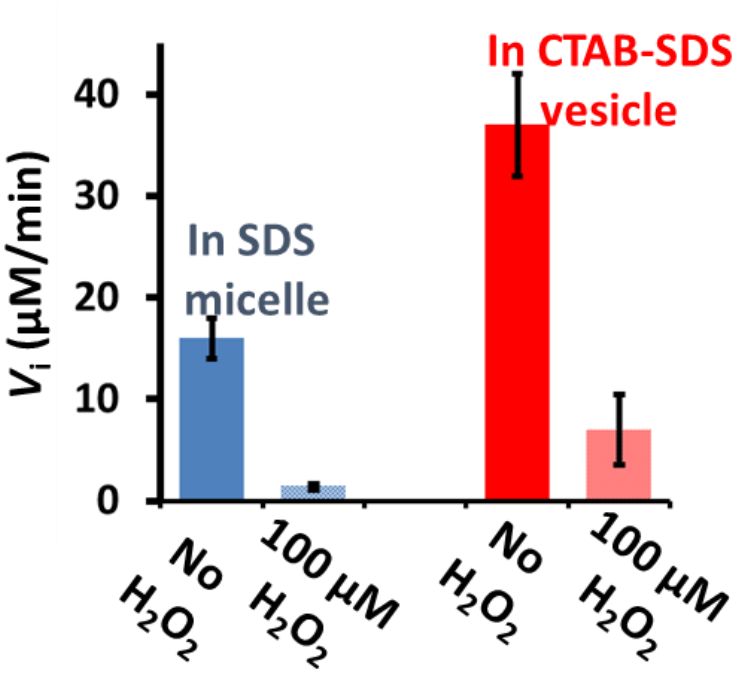

Figure 26: Initial rate (V_i) of KE catalysis of cyt c (5μM) due to the presence of 100μM H_2O_2 at fixed 100 μM NBI concentration under similar experimental conditions in SDS micelles and CTAB-SDS catanionic vesicles.

3.12 Dynamic Light Scattering (DLS) Data:

The hyrodynamic diameter of 20mM SDS with and without cyt c was found to be 6 ± 1 nm and 3 ± 1 nm respectively (as shown in fig. 27 (a)). This clearly suggests that cyt c was attached with SDS micelles (since the increase was similar to cyt c size). The hydrodynamic diameter of DOPC and AOT vesicles were observed to be (100 ± 20 , 600 ± 50) and (200 + 50)nm respectively by DLS technique and Optical microscopic images (fig27 (b) and (d), fig 28 (a) and (b)).

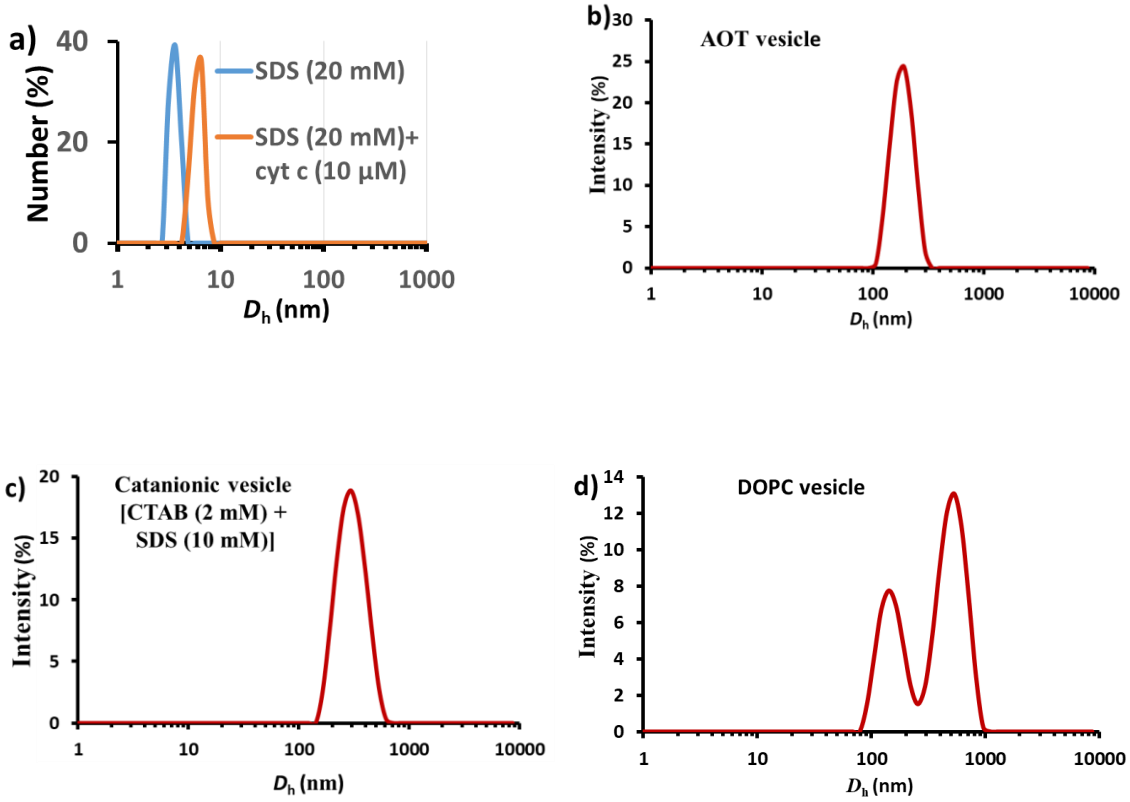

Figure 27: Hydrodynamic diameter of the (a)20mM SDS solution in presence and absence of cyt c (10µM), (b) AOT vesicle, (c) CTAB+SDS catanionic vesicle and (d) DOPC vesicle.

3.13 Microscopic images:

3.13.1 Optical:

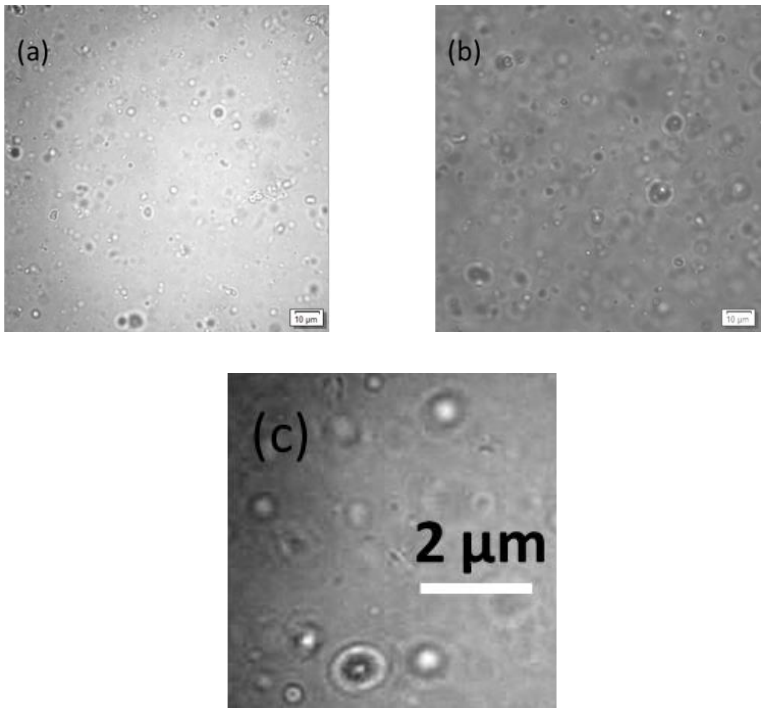

Figure 28: Optical microscopic images of (a) AOT, (b) DOPC vesicles and (c) AOT with cyt c.

3.13.2 Fluorescence:

Fluorescence microscopic image of fluorescein isothiocyanate (FITC)-tagged cyt c with AOT vesicles confirmed binding of the protein.

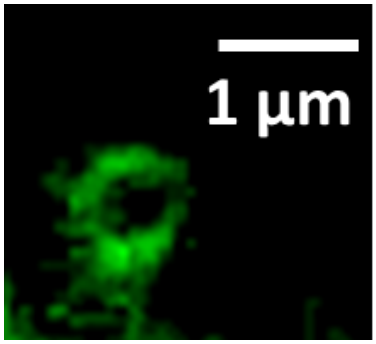

Figure 29: Fluorescence microscopic image of AOT vesicles in presence of cyt c- FITC conjugate.

3.14 TEM images:

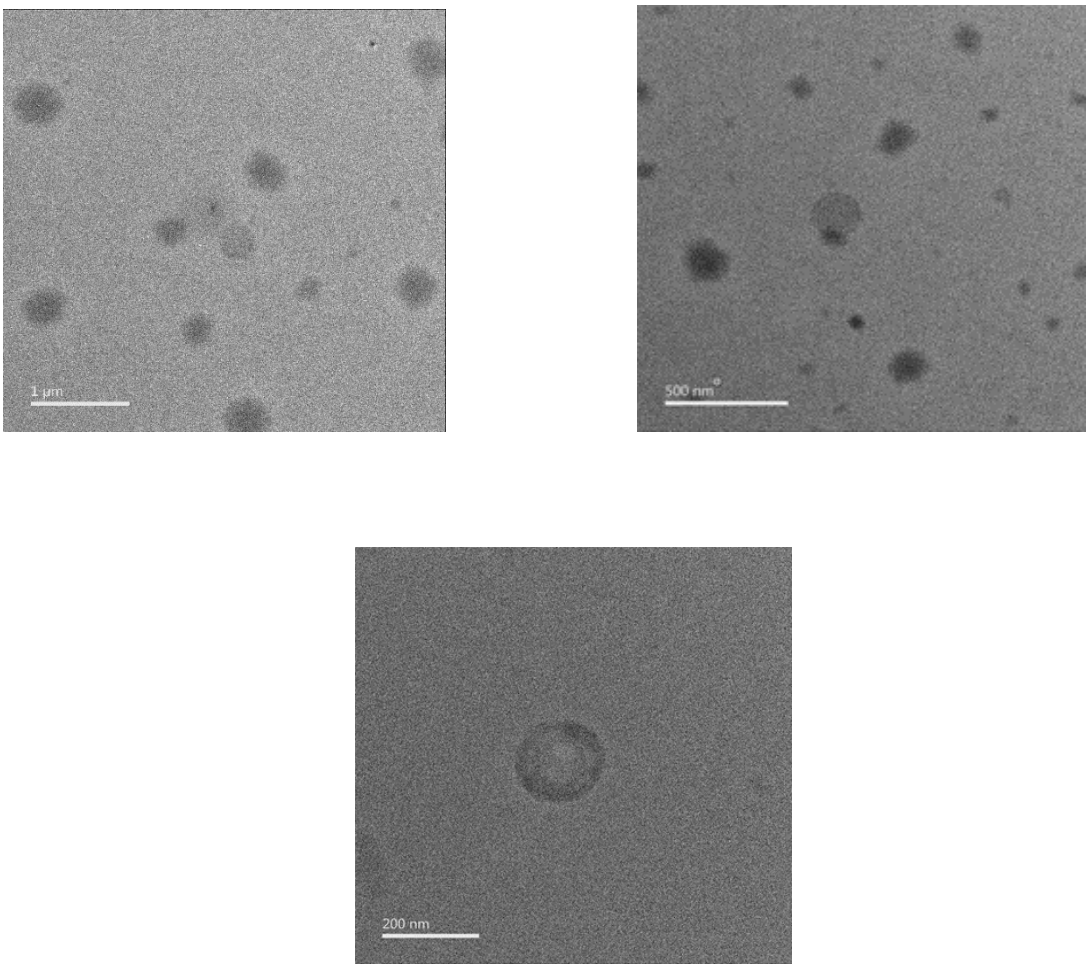

Figure 30: Transmission Electron Microscopic images of CTAB-SDS catanionic micelles (Staining was performed with 1% Phosphomolybdic acid)

3.15 Selective KE catalysis study of cyt c in presence of enzymes/proteins in different media:

Cyt c shows high catalytic activity in SDS micelles and CTAB-SDS catanionic vesicle, selectively. Other enzymes/proteins like Lipase, Alkaline Phosphatase, Haemoglobin, HRP, catalase, lysozyme, BSA were not found to show any activity in micellar or vesicular system whereas, in buffer only BSA shows activity whereas, other enzyme/proteins tested do not.

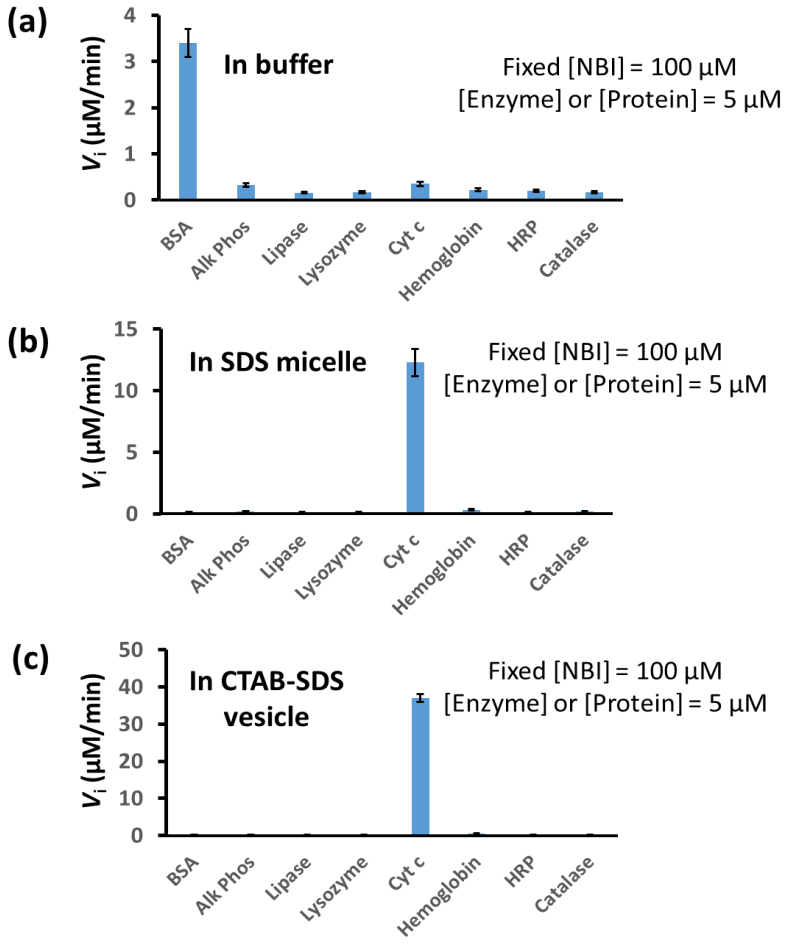

Figure 31: Initial KE catalytic activity of different enzymes/proteins in (a) Buffer, (b) 10 mM SDS and (c) CTAB-SDS catanionic vesicles. Experimental condition: [NBI] = 100 µM, [protein/enzymes] = 5 µM, [CTAB] = 2 mM, [SDS] = 10 mM, phosphate buffer (pH 8, 5 mM).

3.16 Fluorescence Studies:

To understand the reason behind KE catalytic activity by cyt c only restricted to self-organized systems, fluorescence data has been taken which helps in understanding the structural changes that occurs in the cyt c during the reaction. Steady state fluorescence spectra of the protein (by following tryptophan fluorescence at 280nm excitation) is widely used method to understand the protein unfolding [34][35][49]. In native state of the protein the tryptophan fluorescence is quenched by hemin and hence in folded state tryptophan fluorescence is absent. As protein starts getting unfolded tryptophan fluorescence started to unveil because as tryptophan goes away from hemin the quenching effect starts reducing. Figure 32 shows that as the concentration of SDS or CTAB increasing the tryptophan fluorescence intensity is also increasing. In the presence of GDnHCl (guanidium hydrochloride) cyt is completely denatured and hence yield the maximum fluorescence but no KE catalytic effect was observed. Apo cyt c showed the maximum fluorescence, it is due to the absence of hemin therefore no quenching of tryptophan fluorescence was observed in this case. Also no catalytic effect was due to the absence of hydrophobic membrane.

Also denatured cyt c couldn’t recover its KE catalytic activity in SDS micelles, this indicates the importance of secondary structure in micellar and vesicular systems.

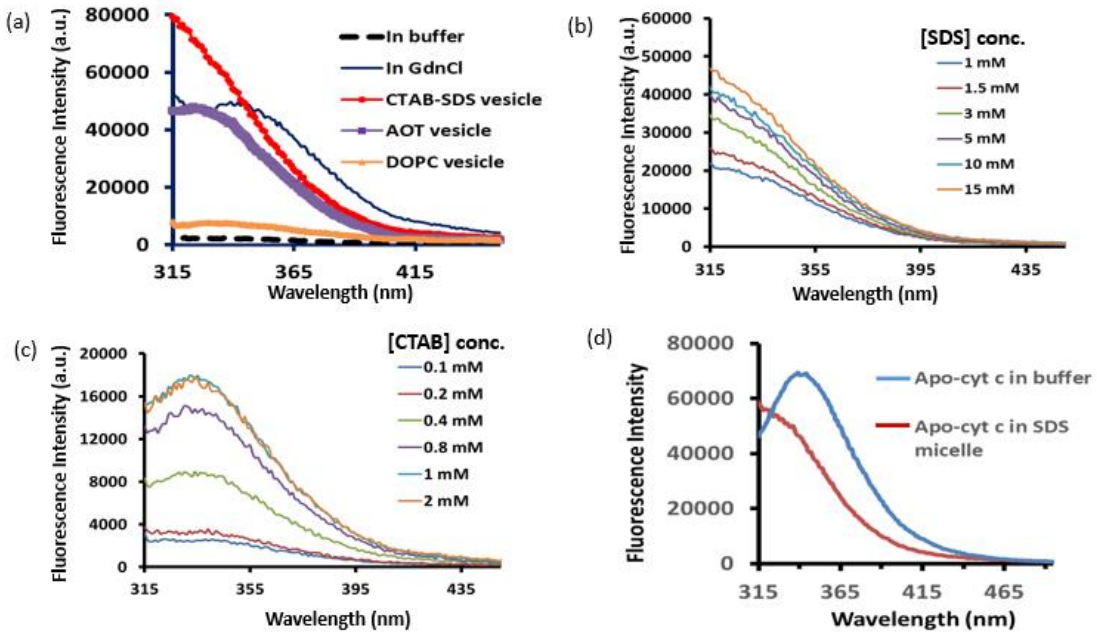

Figure 32: Fluorescence spectrum of cyt c (5 µM) (a) in buffer (phosphate = 5 mM, pH 8), in presence of guanidinium chloride (GdnCl) (6 M), CTAB-SDS catanionic vesicle ([CTAB] = 2 mM, [SDS] = 10 mM), AOT (100 µM) and DOPC (50 µM) vesicle; (b) in presence of different SDS (1-15 mM) and (c) CTAB (0.1-2 mM) concentration. Excitation wavelength = 280 nm, Excitation/Emission slit width = 3/3 nm. (d) Fluorescence spectrum of apo-cyt c (5 µM) in buffer (phosphate = 5 mM, pH 8) and SDS micelle (10 mM). Excitation wavelength = 280 nm, Excitation/Emission slit width = 3/3 nm. Notably, quenching effect of hemin is not here and thus it shows much higher tryptophan fluorescence compared to cyt c.

Residence of protein at hydrophoobic or hydrophilic environment is determined by the ratio of fluorescence intensity at 330 to 350 nm i.e. FI_{330}/FI_{350}[50]. Linear correlation has been found between logarithmic value of Kemp Elimination catalytic activity and unfolding of protein (FI 330 as well as with FI_{330}/FI_{350}). The maximum rate in catanionic vesicles (CTAB-SDS) can be justified on the basis FI_{330}/FI_{350} ratio (1.6) which is maximum in this case among all other systems (as shown in figure 33). In catanionic vesicular medium cyt c is in most hydrophobic region also with highest unfolding (maximum fluorscence intensity).

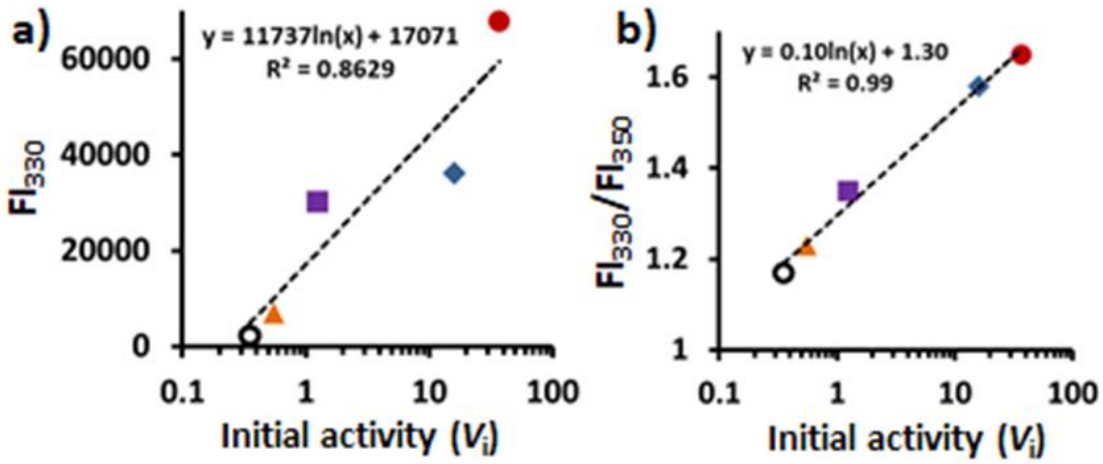

Figure 33: (a) Tryptophan fluorescence intensity (FI) of cyt C (at 330 nm) and (b) Ratio of FI at 330 nm and 350 nm (FI_{330}/FI_{350}) as a function of the initial catalytic rate (V_i) of the proton transfer catalysis in buffer (unfilled black circle), DOPC vesicle (orange triangle), AOT vesicle (purple square), SDS micelle (blue diamond) and CTAB-SDS catanionic vesicle (red circle). Experimental condition: Phosphate buffer (5 mM, pH 8), [SDS] = 10 mM, [CTAB] = 2 mM, [AOT] = 100 µM, [DOPC] = 50 µM, [cyt c] = 5 µM, T = 25 °C.

Similarly, In case of SDS similar trend is obtained between fluorescence values and catalytic rate in different SDS concentration. SDS concentration was varied from 1-15 mM. Linear correlation has been found between logarithmic value of Kemp Elimination catalytic activity and unfolding of protein (FI 330 as well as with FI_{330}/FI_{350}).

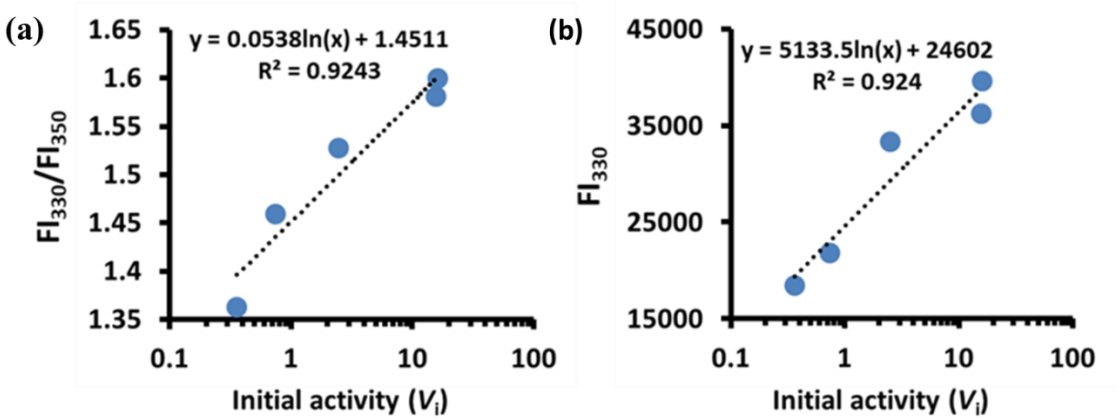

Figure 34: (a) Ratio of FI at 330 nm and 350 nm (FI_{330}/FI_{350}) and (b)Tryptophan fluorescence intensity (FI) of cyt C (at 330 nm) as a function of the initial catalytic rate (V_i) of the proton transfer catalysis at different SDS concentration (1, 3, 5, 10 and 15 mM). Experimental condition: Phosphate buffer (5 mM, pH 8), [cyt c] = 5 µM, T = 25 °C.

3.17 Circular Dichroism study:

CD (Circular Dichroism) data has been taken to understand the structural changes in cyt c. It reveals that in micellar and vesicular systems α-helix increased in all the systems while β-sheet decreased in case of SDS micelles and CTAB-SDS vesicles and increased for AOT and DOPC vesicles in comparison to the buffer.

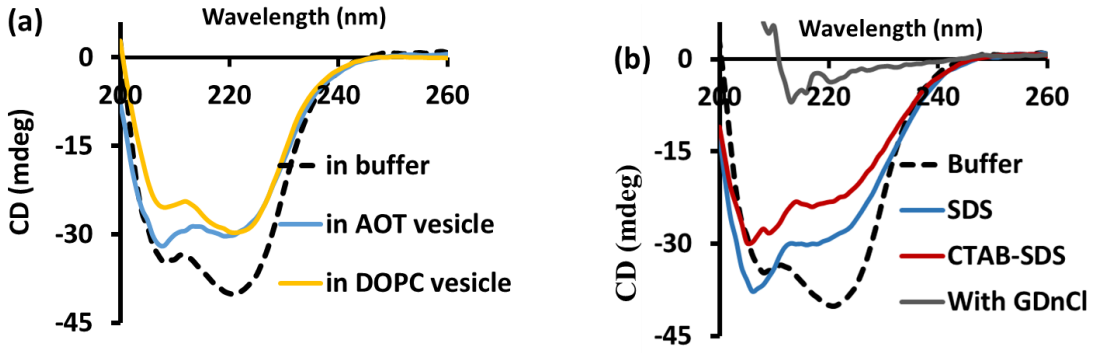

Figure 35: (a) CD spectrum of 20μM cyt c in different systems – (a) buffer, AOT and DOPC vesicle, (b) in 10mM SDS, CTAB –SDS and with GDnHCl (*Guanidium chloride was used 6 M in buffered solution of 20 μM cyt C for CD spectra measurement.)* T = 25 ^{o}C

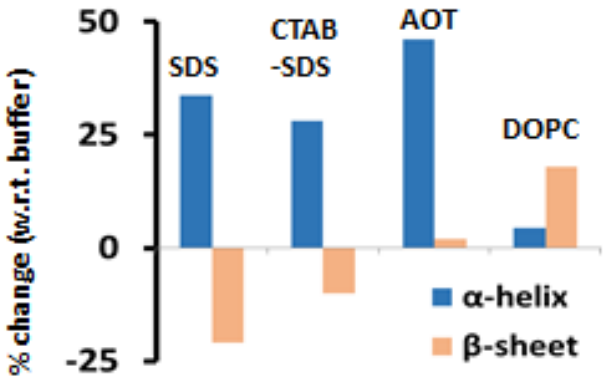

Figure 36: Percentage (%) change in α-helix and β-sheet content of cyt C with respect to buffer. For example, calculation of % change in α-helix content in SDS micelle the following formula has been used: [{(α-helix content)$_{SDS}$-(α-helix content)$_{buffer}$}/ (α-helix content)$_{buffer}$] x 100 (see Table 4 for the values).

Table 4: α-helix and β-sheet content of cyt c in buffer and different self-organized system. (Calculation was done by following reported literature [51])

System	**α-helix**	**β-sheet**
Cyt c in Buffer	8.9 ± 0.2	29.1 ± 2
Cyt c in SDS micelle	11.9 ± 0.3	23 ± 1.5
Cyt c in CTAB-SDS vesicle	11.4 ± 0.5	26.2 ± 1.3
Cyt c in AOT vesicle	13 ± 0.6	29.7 ± 1.9
Cyt c in DOPC vesicle	9.3 ± 0.3	34.3 ± 2.9

3.18 UV-Vis experiment with diphenyl-1,3,5-hexatriene (DPH)

The solubility of a hydrophobic probe, DPH, was measured in different systems by performing UV-Vis scans. It was found that DPH was maximum soluble in CTAB-SDS vesicle compared to micellar system having similar amount of surfactant since the former has the highest hydrophobicity amongst all other systems. DPH is known to display characteristics UV peak 350, 360 and 373 nm once it get solubilized in hydrobhobic environment.[52]

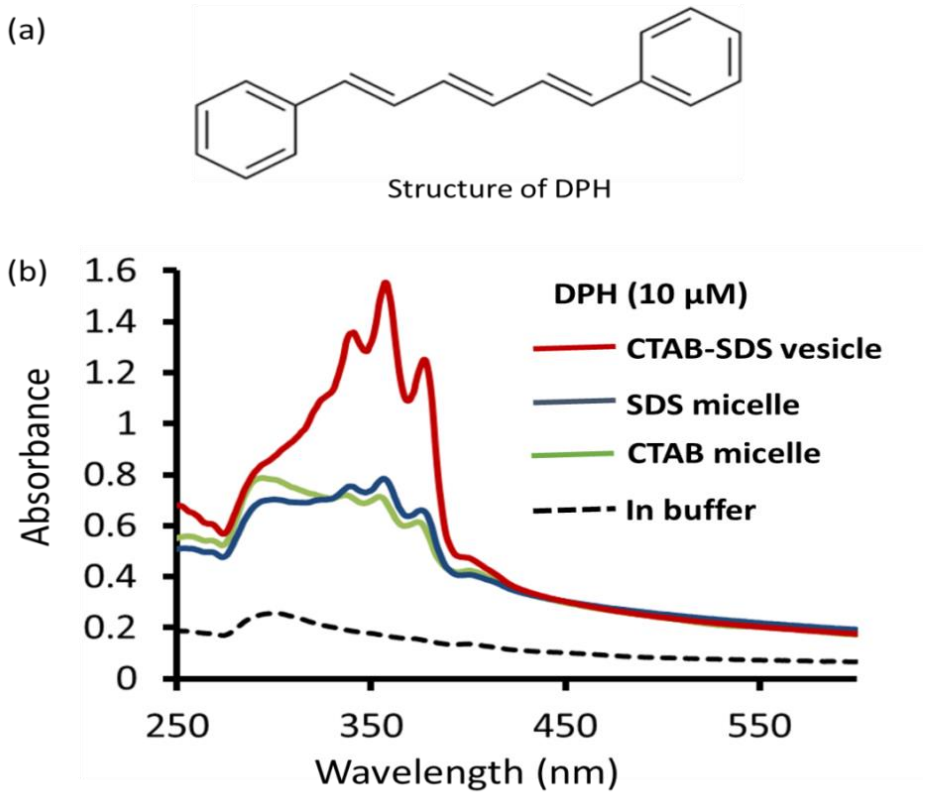

Figure 37: (a) Structure of DPH (b) UV-Vis scan spectra for DPH in CTAB-SDS vesicle, SDS micelle, CTAB micelle and buffer.

3.19 KE catalytic activity of hemin in buffer and SDS micelles:

Activity with only hemin in buffer and SDS micelle was also checked but no significant activity was observed.

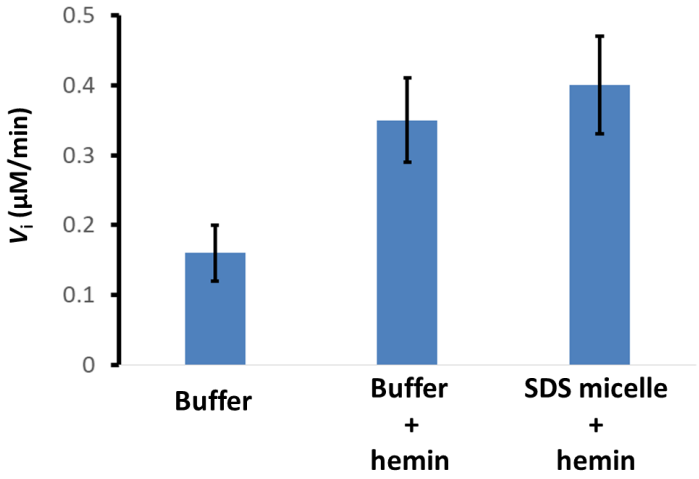

Figure 38: Initial KE catalytic activity of hemin in buffer and 10 mM SDS micelle. Experimental condition: [NBI] = 100 µM, [hemin] = 10 µM, phosphate buffer (pH 8, 5 mM).

3.20 Percentage (%) decrease in rate by modified cyt c and BSA:

Figure 39 shows the percentage (%) decrease in initial rate of KE catalysis by modified protein as compared to native protein. FITC is known to bind with lysine residue of BSA[46] which results in almost 90% decrease in rate . FITC tagged cyt c didn't showed any decrement in rate, this shows that lysine residue in cyt c is not responsible for proton transfer catalysis. Apo cyt c showed almost 100% reduction in rate, this implies hemin plays very important role in the catalysis. It is known that DEPC binds with histidine[53] , cyt c-DEPC showed approx. 80 % decrease in the rate, this shows that histidine plays very important role in the catalysis.

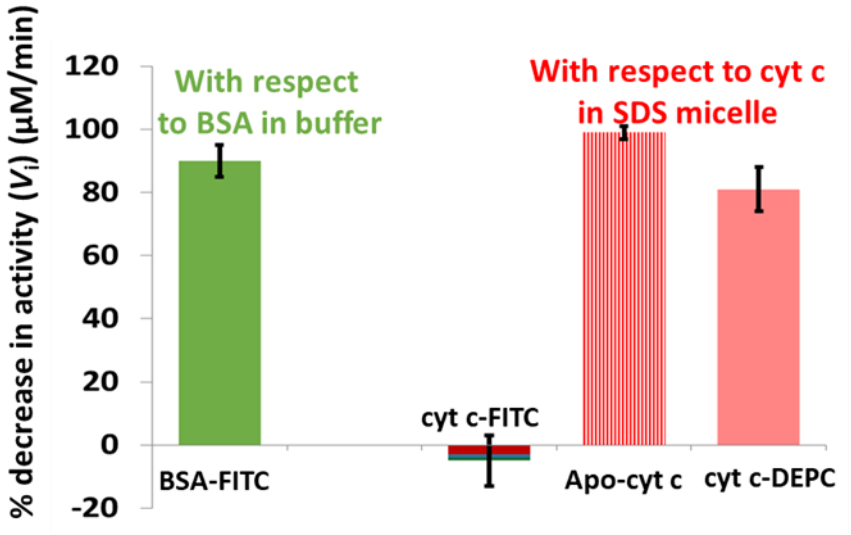

Figure 39: Percentage (%) decrease in initial rate (Vi) of KE catalysis (in comparison to the native protein and modified protein) due to tagging of FITC in BSA, in cyt c, removal of hemin group (i.e. apo cyt c) and due to tagging of ethanoate group in the histidine moiety (due to the reaction with DEPC) at fixed substrate (NBI=100µM) in presence of 5µM cyt c.

3.21 Kinetics of cyt c in presence of diethylpyrocarbonate (DEPC) in different systems:

We assumed that histidine moiety (His-18) of cyt c co-ordinated proximally to hemin may well act as the base to initiate proton elimination with the hemin coordinated benzisoxazole substrate[54]. The hemin coordination of KE substrate has been reported in earlier literature[55]. The role of proximal hemin was studied by covalent modification of imidazole NH of histidine by DEPC. The binding of DEPC with cyt c histidine was verified by UV-vis (Figure 42, 43 and 44) and CD spectroscopy (Figure 45).

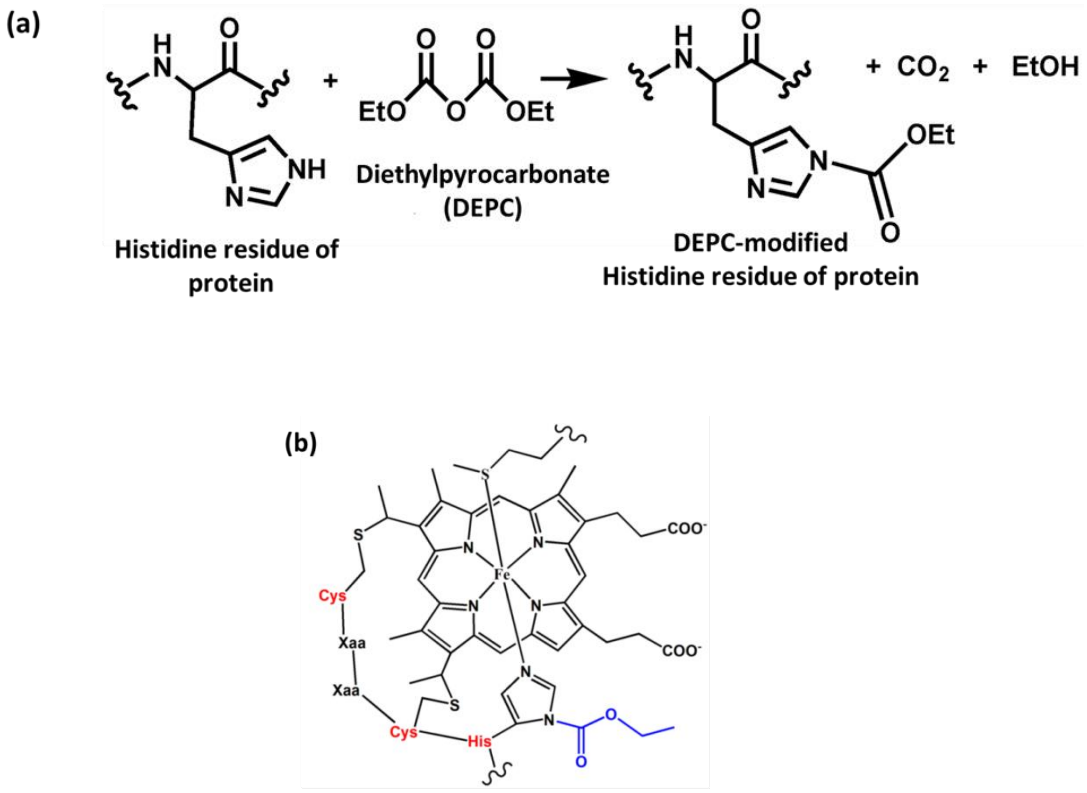

Figure 40: (a) Schematic of the reaction to show the DEPC modification of the histidine residue of protein. (b) Schematic representation of the tagging of ehtanoate group of DEPC with histidine (His-18) of cyt c near to hemin group.

Figure 41 (a) and (b) shows that there is significant decrease in KE catalytic rate by cyt c with increasing DEPC concentration. We can observe that 2 mM DEPC diminished the KE catalytic rate of cyt c by ~ 90% and~30% in SDS micelles and CTAB-SDS catanionic vesicles respectively. The IC_{50} value of DEPC inhibition on cyt c activity in SDS micelles and CTAB-SDS catanionic vesicles were found to be 0.28 and 3.8 mM, respectively.

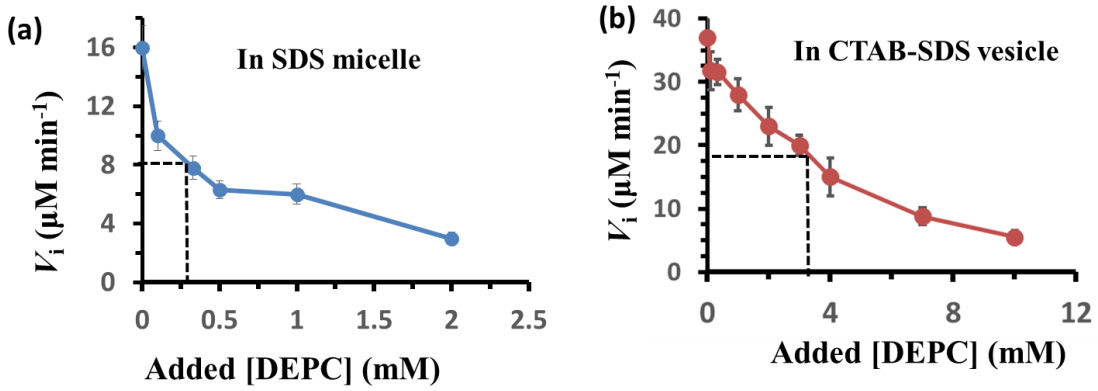

Figure 41: Plot of initial catalytic rate (V_i) in presence of different concentration of DEPC in (a) 10 mM SDS and (b) CTAB-SDS vesicle. Dotted lines showed the 50% inhibited activity was obtained at 0.3 µM (for SDS micelles) and 3.2 µM (for CTAB-SDS vesicles) addition of DEPC.

Fig. 42 (b) shows, a gradually generated peak (at 242 nm) with time due to the increase in binding of DEPC to imidazole NH of histidine, which is more prominent in case of SDS micelles than in buffer. This rise in UV absorbance at 242 nm is a characteristics of DEPC-tagging with histidine[53].

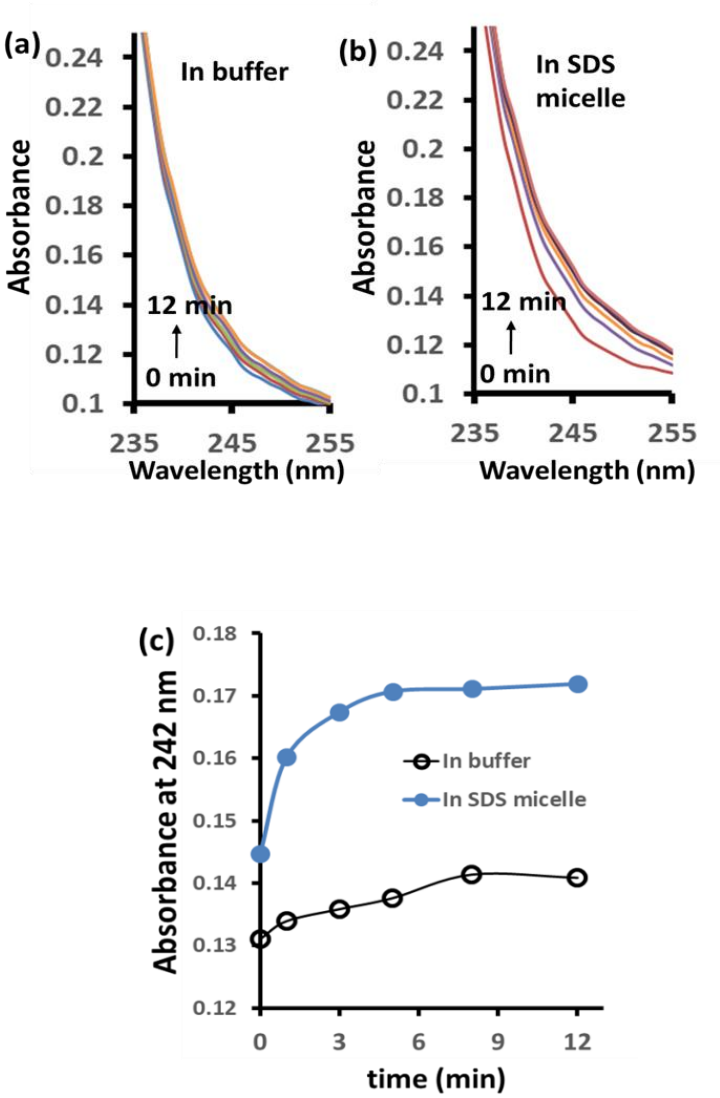

Figure 42: UV-vis scan spectra of DEPC + cyt c in (a) buffer and (b) 10 mM SDS micelles. (c) Absorbance at 242nm of DEPC + cyt c as a function of time in buffer and 10mM SDS micelles. [DEPC] = 2 mM, [cyt c] = 5 µM, phosphate buffer (pH 8, 5 mM).

Figure 43 shows a gradual blue shift of the soret peak from 407 nm to 399 nm in SDS micelles and CTAB-SDS catanionic vesicles, whereas in buffer this was not observed, which confirms the binding of DEPC to the histidine moiety[53].

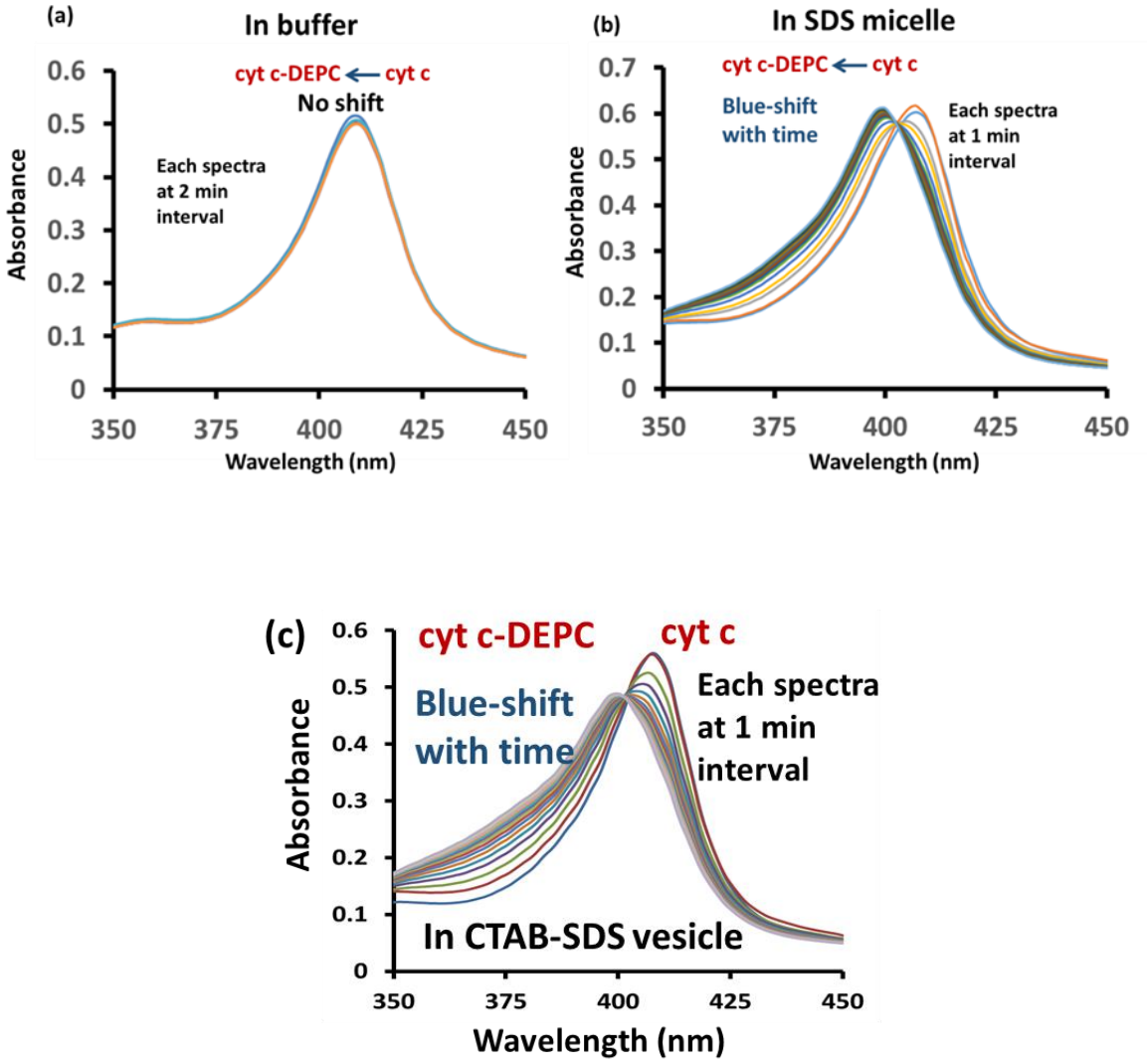

Figure 43: UV-vis scan of DEPC-cyt c recorded for 12 minutes with 1min interval in (a) buffer and (b) SDS micelle. (c) CTAB-SDS catanionic vesicles. [cyt c] = 5 µM, [DEPC] = 2 mM, phosphate buffer (pH 8, 5 mM)

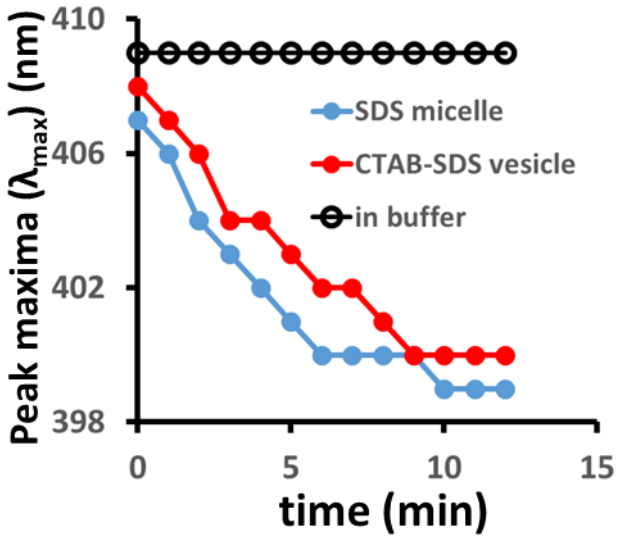

Figure 44: Gradual change in soret peak maxima with time due to binding of DEPC in cyt c in buffer, SDS micelle and CTAB-SDS vesicle. [cyt c] = 5 µM, [DEPC] = 2 mM, phosphate buffer (pH 8, 5 mM).

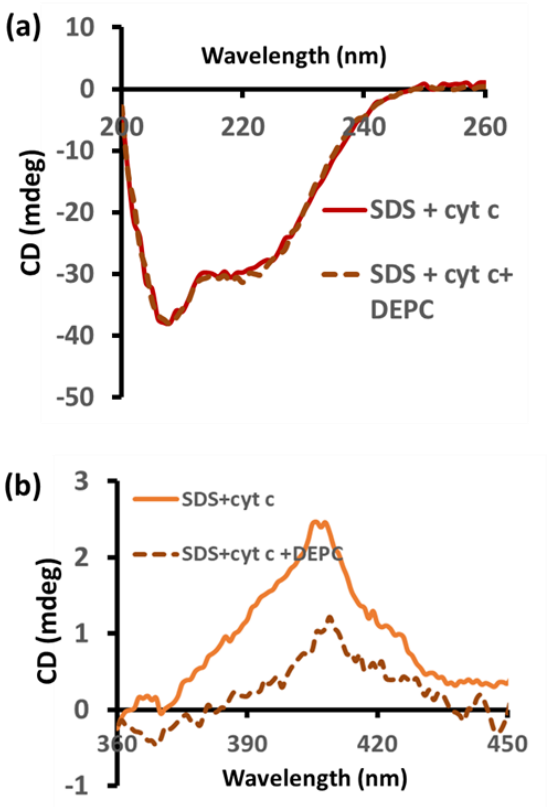

Figure 45: CD spectra of cyt c (a) in near UV region (200-260 nm), (b) in Soret region (360-450 nm) in SDS micelle in absence and presence of DEPC (2 mM). [SDS] = 10 mM, [cyt c] = 20 µM, phosphate buffer (pH 8, 5 mM).

Chapter 4

Conclusions

Here we have found unprecedented catalytic promiscuous property of cyt c, which is strictly restricted to membrane mimetic media like micelles and vesicles. Also, the best catalytic activity with cyt c was found to be in CTAB-SDS catanionic vesicular system than in SDS micellar system (3 fold higher activity in CTAB-SDS catanionic vesicular system than SDS micellar system under similar reaction conditions), it is due to high hydrophobicity of catanionic vesicular system than micellar system which is confirmed by the DPH (a hydrophobic probe). Rate of the reaction in CTAB-SDS catanionic vesicular system by cyt c is found to be 2.5 fold higher than other natural biocatalyst Bovine Serum Albumin (BSA).This unusual property strengthens the claim that early developed proteins/enzymes typically have wide substrate specificity to perform multiple tasks in early life forms as compared to lately developed enzymes in evolutionary processes.

The catalytic rate was found to be reduced by ~80% as we tagged DEPC to cyt c (DEPC is known to bind with histidine), this shows that histidine might play important role in the KE catalysis. Also this cyt c catalysis is pH dependent, the rate is drastically decreased below pH 6, which suggests that base catalysed mechanism might be involved in the catalysis and probably proximal histidine (near heme) is acting as base for the abstraction of proton from NBI to form 2-CNP.

This study exemplifies the versality and emergent behaviour of biomolecules in response to its surrounding environment which also reinforce the possibility of dramatic amendment of bio catalytic properties in confined space[56][57].

References:

[1] Y. Stone and N. Park, “Chapter 1,” pp. 1–9.

[2] P. E. V. Paul, V. Sangeetha, and R. G. Deepika, *Emerging Trends in the Industrial Production of Chemical Products by Microorganisms*. Elsevier Inc., 2019.

[3] M. Svedendahl and P. Berglund, “Biocatalytic Promiscuity,” pp. 3391–3401, 2011, doi: 10.1002/ejoc.201001664.

[4] R. A. Jensen, “Enzyme recruitment in evolution of new function .;.1687,” 1976.

[5] P. J. O. Brien and D. Herschlag, “Patrick J O’Brien,” no. April, 1999.

[6] O. Khersonsky, C. Roodveldt, and D. S. Tawfik, “Enzyme promiscuity : evolutionary and mechanistic aspects,” doi: 10.1016/j.cbpa.2006.08.011.

[7] A. Babtie, N. Tokuriki, and F. Hollfelder, “What makes an enzyme promiscuous ?,” *Curr. Opin. Chem. Biol.*, vol. 14, no. 2, pp. 200–207, 2010, doi: 10.1016/j.cbpa.2009.11.028.

[8] O. Khersonsky and D. S. Tawfik, “Enzyme Promiscuity : A Mechanistic and Evolutionary Perspective,” 2010, doi: 10.1146/annurev-biochem-030409-143718.

[9] M. Soskine and D. S. Tawfik, “Mutational effects and the evolution of new protein functions,” *Nat. Publ. Gr.*, vol. 11, no. 8, pp. 572–582, 2010, doi: 10.1038/nrg2808.

[10] S. D. Copley, “Enzymes with extra talents : moonlighting functions and catalytic promiscuity,” pp. 265–272, doi: 10.1016/S1367-5931(03)00032-2.

[11] I. Nobeli, A. D. Favia, and J. M. Thornton, “review Protein promiscuity and its implications for biotechnology,” vol. 27, no. 2, pp. 157–167, 2009, doi: 10.1038/nbt1519.

[12] K. Hult and P. Berglund, “Enzyme promiscuity: mechanism and applications,” *Trends Biotechnol.*, vol. 25, no. 5, pp. 231–238, 2007, doi: 10.1016/j.tibtech.2007.03.002.

[13] T. L. O. Loughlin and W. M. Patrick, “Natural history as a predictor of protein evolvability,” vol. 19, no. 10, pp. 439–442, 2006, doi: 10.1093/protein/gzl029.

[14] A. E. Todd, C. A. Orengo, and J. M. Thornton, “Evolution of Function in Protein Superfamilies , from a Structural Perspective,” 2001, doi: 10.1006/jmbi.2001.4513.

[15] M. Höhne, S. Schätzle, H. Jochens, K. Robins, and U. T. Bornscheuer, “guides in silico enzyme identification,” *Nat. Chem. Biol.*, vol. 6, no. NOVEMBER, 2010, doi: 10.1038/nchembio.447.

[16] N. J. Turner, “Directed evolution drives the next generation of biocatalysts,” vol. 5, no. 8, 2009, doi: 10.1038/nchembio.203.

[17] C. K. Savile, “Biocatalytic Asymmetric Synthesis of,” vol. 305, no. 2010, 2012, doi: 10.1126/science.1188934.

[18] F. H. Arnold, “The nature of chemical innovation: New enzymes by evolution,” *Q. Rev. Biophys.*, vol. 48, no. 4, pp. 404–410, 2015, doi: 10.1017/S003358351500013X.

[19] A. Aharoni, L. Gaidukov, O. Khersonsky, S. M. Gould, C. Roodveldt, and D. S. Tawfik, “The ‘ evolvability ’ of promiscuous protein functions,” vol. 37, no. 1, pp. 73–76, 2005, doi: 10.1038/ng1482.

[20] R. B. Leveson-Gower, C. Mayer, and G. Roelfes, “The importance of catalytic promiscuity for enzyme design and evolution,” *Nat. Rev. Chem.*, vol. 3, no. 12, pp. 687–705, 2019, doi: 10.1038/s41570-019-0143-x.

[21] Q. Wu, B. Liu, and X. Lin, “Current Organic Chemistry, 2010,14,1966-1988 (Review de promiscuidad catalitica de Lin).pdf,” pp. 1966–1988, 2010.

[22] M. T. Reetz, “Directed Evolution of Artificial Metalloenzymes: A Universal Means to Tune the Selectivity of Transition Metal Catalysts?,” *Acc. Chem. Res.*, 2019, doi: 10.1021/acs.accounts.8b00582.

[23] O. F. Brandenberg, K. Chen, and F. H. Arnold, “Directed Evolution of a Cytochrome P450 Carbene Transferase for Selective Functionalization of Cyclic Compounds,” *J. Am. Chem. Soc.*, vol. 141, no. 22, pp. 8989–8995, 2019, doi: 10.1021/jacs.9b02931.

[24] “11directed evolution of gene.pdf.” .

[25] C. Zeymer and D. Hilvert, “Directed Evolution of Protein Catalysts,” *Annu. Rev. Biochem.*, vol. 87, no. 1, pp. 131–157, 2018, doi: 10.1146/annurev-biochem-062917-012034.

[26] R. K. Zhang, K. Chen, X. Huang, L. Wohlschlager, H. Renata, and F. H. Arnold, “Enzymatic assembly of carbon–carbon bonds via iron-catalysed sp 3 C–H functionalization,” *Nature*, vol. 565, no. 7737, pp. 67–72, 2019, doi: 10.1038/s41586-018-0808-5.

[27] D. C. M. Albanese and N. Gaggero, “Albumin as a promiscuous biocatalyst in organic synthesis,” *RSC Adv.*, vol. 5, no. 14, pp. 10588–10598, 2015, doi: 10.1039/c4ra11206g.

[28] K. Kikuchi, S. N. Thorn, and D. Hilvert, “Albumin-catalyzed proton transfer,” *J. Am. Chem. Soc.*, vol. 118, no. 34, pp. 8184–8185, 1996, doi: 10.1021/ja9617395.

[29] G. Boucher *et al.*, “Serum albumin-catalyzed trigger system by using a tandem kemp elimination/β-elimination reaction,” *ChemBioChem*, vol. 6, no. 5, pp. 807–810, 2005, doi: 10.1002/cbic.200400255.

[30] Y. Miao, R. Metzner, and Y. Asano, “Kemp Elimination Catalyzed by Naturally Occurring Aldoxime Dehydratases,” *ChemBioChem*, vol. 18, no. 5, pp. 451–454, 2017, doi: 10.1002/cbic.201600596.

[31] T. Yamanaka, “Cytochrome c and evolution,” *Nature*, vol. 213, no. 5082, pp. 1183–1186, 1967, doi: 10.1038/2131183a0.

[32] B. Kadenbach, “Introduction to Mitochondrial Oxidative,” *Adv. Exp. Med. Biol.*, vol. 748, no. June 2012, pp. 1–11, 2012, doi: 10.1007/978-1-4614-3573-0.

[33] M. Hüttemann *et al.*, “NIH Public Access,” vol. 11, no. 3, pp. 369–381, 2012, doi: 10.1016/j.mito.2011.01.010.The.

[34] N. A. Belikova *et al.*, “Peroxidase activity and structural transitions of cytochrome c bound to cardiolipin-containing membranes,” *Biochemistry*, vol. 45, no. 15, pp. 4998–5009, 2006, doi: 10.1021/bi0525573.

[35] S. Maiti, K. Das, S. Dutta, and P. K. Das, “Striking improvement in peroxidase

activity of cytochrome c by modulating hydrophobicity of surface-functionalized gold nanoparticles within cationic reverse micelles," *Chem. - A Eur. J.*, vol. 18, no. 47, pp. 15021–15030, 2012, doi: 10.1002/chem.201202398.

[36] K. R. Benson, J. Gorecki, A. Nikiforov, W. Tsui, R. M. Kasi, and C. V. Kumar, "Cytochrome: C -poly(acrylic acid) conjugates with improved peroxidase turnover number," *Org. Biomol. Chem.*, vol. 17, no. 16, pp. 4043–4048, 2019, doi: 10.1039/c9ob00541b.

[37] E. Sanchez, S. Lu, C. Reed, J. Schmidt, and M. Forconi, "Kemp elimination in cationic micelles: Designed enzyme-like rates achieved through the addition of long-chain bases," *J. Phys. Org. Chem.*, vol. 29, no. 4, pp. 185–189, 2016, doi: 10.1002/poc.3515.

[38] P. Gomez-Tagle, I. Vargas-Zúñiga, O. Taran, and A. K. Yatsimirsky, "Solvent effects and alkali metal ion catalysis in phosphodiester hydrolysis," *J. Org. Chem.*, vol. 71, no. 26, pp. 9713–9722, 2006, doi: 10.1021/jo061780i.

[39] M. L. Casey, D. S. Kemp, K. G. Paul, and D. D. Cox, "The Physical Organic Chemistry of Benzisoxazoles. I. The Mechanism of the Base-Catalyzed Decomposition of Benzisoxazoles," *J. Org. Chem.*, vol. 38, no. 13, pp. 2294–2301, 1973, doi: 10.1021/jo00953a006.

[40] B. Tah, P. Pal, and G. B. Talapatra, "Interaction of insulin with SDS/CTAB catanionic Vesicles," *J. Lumin.*, vol. 145, pp. 81–87, 2014, doi: 10.1016/j.jlumin.2013.07.040.

[41] P. Andreozzi *et al.*, "Multi- to unilamellar transitions in catanionic vesicles," *J. Phys. Chem. B*, vol. 114, no. 24, pp. 8056–8060, 2010, doi: 10.1021/jp100437v.

[42] A. Shome, T. Kar, and P. K. Das, "Spontaneous formation of biocompatible vesicles in aqueous mixtures of amino acid-based cationic surfactants and SDS/SDBS," *ChemPhysChem*, vol. 12, no. 2, pp. 369–378, 2011, doi: 10.1002/cphc.201000708.

[43] "44 aot dopc vesicles.pdf." .

[44] P. Andreozzi *et al.*, "Multi- to Unilamellar Transitions in Catanionic Vesicles,"

vol. 1, pp. 8056–8060, 2010.

[45] C. Sun, B. Hu, W. Zhou, S. Xu, and Z. Liu, “Investigations on the demetalation of metalloporphyrins under ultrasound irradiation,” *Ultrason. Sonochem.*, vol. 18, no. 2, pp. 501–505, 2011, doi: 10.1016/j.ultsonch.2010.08.010.

[46] N. Barbero, C. Barolo, and G. Viscardi, “Bovine Serum Albumin Bioconjugation with FITC,” *World J. Chem. Educ. Vol. 4, 2016, Pages 80-85*, vol. 4, no. 4, pp. 80–85, 2016, doi: 10.12691/WJCE-4-4-3.

[47] B. Anfinsen, “From the Laboratory of Chemical Biology, National Institute of Arthritis, National Institutes of Health, Bethesda, Maryland %‘OOlJ Metabolism and Digestive Diseases,” *J. Biol. Chem.*, no. 9, pp. 3188–3195, 1973.

[48] F. Hollfelder, A. J. Kirby, and J. B. F. N. Engberts, “Vesicles Accelerate Proton Transfer from Carbon up to 850-fold,” vol. 2, no. 6, 2000.

[49] N. Sanghera and T. J. T. Pinheiro, “Unfolding and refolding of cytochrome c driven by the interaction with lipid micelles,” pp. 1194–1202, 2000.

[50] P. Dogra, A. Joshi, A. Majumdar, and S. Mukhopadhyay, “Intermolecular charge-transfer modulates liquid- liquid phase separation and liquid-to-solid maturation of an intrinsically disordered pH-responsive domain Abstract Liquid-liquid phase separation of intrinsically disordered proteins into mesoscopic , dynamic ,” 2019.

[51] F. Wien, J. Kun, Y. Lee, Y. Goto, and R. Matthieu, “BeStSel : a web server for accurate protein secondary structure prediction and fold recognition from the circular dichroism spectra Andr as,” vol. 46, no. July, pp. 315–322, 2018, doi: 10.1093/nar/gky497.

[52] M. T. M. António, J. R. Robalo, P. D. Santos, A. J. Palace, J. P. P. Ramalho, and L. M. S. Loura, “Biochimica et Biophysica Acta Diphenylhexatriene membrane probes DPH and TMA-DPH : A comparative molecular dynamics simulation study,” *BBA - Biomembr.*, vol. 1858, no. 11, pp. 2647–2661, 2016, doi: 10.1016/j.bbamem.2016.07.013.

[53] D. Khananshvili, “Modification of histidine residues by diethyl pyrocarbonate leads to inactivation of the Rhodospirillum rubrum RrFl-ATPase,” vol. 159, no. 1,

pp. 271–274, 1983.

[54] C. Metallomics, J. G. Kleingardner, and K. L. Bren, “Metallomics Comparing substrate specificity between cytochrome c maturation and cytochrome c heme lyase systems for cytochrome c biogenesis w,” pp. 396–403, 2011, doi: 10.1039/c0mt00086h.

[55] A. Kemp *et al.*, “A redox-mediated Kemp eliminase,” *Nat. Commun.*, pp. 1–8, 2017, doi: 10.1038/ncomms14876.

[56] A. Küchler, M. Yoshimoto, S. Luginbühl, F. Mavelli, and P. Walde, “Enzymatic reactions in confined environments,” *Nat. Publ. Gr.*, vol. 11, no. 5, pp. 409–420, 2016, doi: 10.1038/nnano.2016.54.

[57] L. J. Prins, “Emergence of Complex Chemistry on an Organic Monolayer,” 2015, doi: 10.1021/acs.accounts.5b00173.